PB-227 506

SIGNIFICANCE OF COMBUSTION NUCLEI TO AIR POLLUTION

J. E. Quon

Northwestern University
Evanston, Illinois

September 1971

DISTRIBUTED BY:

NTIS

National Technical Information Service
U. S. DEPARTMENT OF COMMERCE
5285 Port Royal Road, Springfield Va. 22151

PB 227 506

Northwestern University
The Technological Institute
Evanston, Ill., 60201

Significance of Combustion Nuclei to Air Pollution

by

J. E. Quon

Principle Investigator

Reproduced by
NATIONAL TECHNICAL
INFORMATION SERVICE
U S Department of Commerce
Springfield VA 22151

Final Report

Office of Air Programs
Research Grant AP-00039
Environmental Protection Agency

Grant Period: Oct., 1966 - Sept., 1969
(no cost extension to Nov., 1970)

September, 1971

79

TABLE OF CONTENTS

Page

INTRODUCTION..... 1

SECTION I..... 3

Coagulation of a Continuously Reinforced Aerosol

General
Aerosol Model
Results and Discussion
References
Figures 1 to 6
Table 1

SECTION II..... 24

Particle Formation From Photooxidation of Sulfur Dioxide in Air

General
Experimental Apparatus and Procedures
Results and Discussion
References
Notations
Figures 1 and 2
Tables 1 to 8

SECTION III..... 49

A Spark Replica Technique for the Measurement of Sulfuric Acid Nuclei

General
Experimental Apparatus and Procedures
Results and Discussion
References
Figures 1 to 10
Tables 1 and 2

LIST OF FIGURES

Figure	Title	Page
SECTION I		
1.	Particle Concentration as a Function of Time and Size Parameters: $K_{ij} = 1$, $I_1 = 1$; K_{ij}, $(\lambda/r_1) = 0$, $I_1 = 1$; K_{ij}, $(\lambda/r_1) = 1$, $I_1 = 1$.	17
2.	Particle Concentration as a Function of Time and Size Parameters: K_{ij}, $(\lambda/r_1) = 0$, I_k; K_{ij}, $(\lambda/r_1) = 1$, I_k.	18
3.	Particle Concentration versus Size for Different Values of the Time Parameter τ: $K_{ij} = 1$ and $I_1 = 1$.	19
4.	Particle Concentration versus Size for Different Values of the Time Parameter τ: $K_{ij} = 1$ and I_k.	20
5.	Particle Concentration versus Size for Different Values of the Time Parameter τ: K_{ij}, $(\lambda/r_1) = 0$, I_k; K_{ij}, $(\lambda/r_1) = 1$, I_k.	21
6.	Particle Concentration versus Size for Different Values of the Time Parameter τ: K_{ij}, $(\lambda/r_1) = 0$, $I_1 = 1$; K_{ij}, $(\lambda/r_1) = 1$, $I_1 = 1$.	22
SECTION II		
1.	Nuclei Concentration vs Irradiation Time	39
2.	Nuclei Concentration vs Initial Sulfur Dioxide Concentration	40
SECTION III		
1.	Schematic Diagram of the Spark Replica Counter.	62
2.	Electric Circuit Diagram of the Spark Replica Counter.	63
3.	Spark Count as a Function of the Voltage Gradient.	64
4.	Spark Count as a Function of Etching Time, With Stirring.	65

SECTION III (Continued)

Figure	Title	Page
5.	Spark Count as a Function of Etching Time, Without Stirring.	66
6.	Schematic Diagram of the Sampling System.	67
7.	Effect of Sample Flow Rate on Spark Count.	68
8.	Effect of Sample Volume on Spark Count.	69
9.	Nuclei Concentration vs. Spark Count.	70
10.	Nuclei Concentration vs. Spark Count, Aggregated Basis.	71

LIST OF TABLES

Table	Title	Page
SECTION I		
1.	Comparison of Numerical Computations with Analytical Solutions	23
SECTION II		
1.	Nuclei Concentration vs Irradiation Time (Relative Humidity 13-19%, $(SO_2)_o$ = 0.202 ppm)	41
2.	Nuclei Concentration vs Irradiation Time (Relative Humidity 41-43%, $(SO_2)_o$ = 0.202 ppm)	42
3.	Nuclei Concentration vs Irradiation Time (Relative Humidity 53-60%, $(SO_2)_o$ = 0.202 ppm)	43
4.	Nuclei Concentration vs Irradiation Time (Relative Humidity 70-77%, $(SO_2)_o$ = 0.202 ppm)	44
5.	Nuclei Concentration vs Time (Relative Humidity 49-55%, $(SO_2)_o$ = 0.647 ppm)	45
6.	Nuclei Concentration vs Initial Sulfur Dioxide Concentration (Relative Humidity 13-19%, Irradiation Time = 60 sec)	46
7.	Nuclei Loss Through Filtration	47
8.	Nuclei Loss Through Diffusion Tubes (Air Flow 3 ℓ/min)	48
SECTION III		
1.	Etching Characteristics of Plastic Films	72
2.	Sulfuric Acid Nuclei Concentration vs. Spark Count.	73

INTRODUCTION

The particle size distribution and concentration of an aerosol are influenced by coagulation, sedimentation, the rate of generation of particles, particle characteristics and the dynamics of the fluid in which the particles are suspended. The air pollution specialist is interested in the description of particle concentration and size distribution and in how they are interdependent on the physical and chemical processes occurring in the urban atmosphere. The research reported here provides information leading to an improved description of and understanding of the aerosol in the polluted atmosphere.

The aerosol model incorporating the feature of continuous reinforcement is the first of such models to be proposed for the behavior of aerosols in the polluted atmosphere. The analysis of this model affords some insight into the dependence of size distribution on the rate of reinforcement.

The reinforcement of aerosols in the atmosphere may arise from emission of particles to the atmosphere by natural processes and the many activities of man, and/or may arise from the formation of particles in situ from heterogeneous gas-particle or homogeneous gaseous reactions. For the situation where generation of particles in situ is the result of photooxidation of organic and/or inorganic gases or vapors, the maximal initial concentrations of reactants consistent with some predetermined rate of formation of submicron particles is of interest to the air pollution control field. For the situation where the rate of particle formation is known, analysis of the reinforced aerosol model to give an estimate of the gross particulate weight concentration is of interest. Both types of information may serve as guidelines for suggesting air quality standards.

The association of sulfur dioxide with adverse health effects has been

documented by statistical methods of inference. These methods, of course, do not prove the existence of a cause and effect relationship. While considerable attention has been focused on sulfur dioxide as a result of these statistical correlations, comparatively little attention has been given to the measurement of sulfuric acid in the urban atmosphere and its implications to public health. However, the toxicity of sulfuric acid is known to be greater than that of sulfur dioxide. It is also known that the reaction product of the photooxidation of sulfur dioxide in air is sulfuric acid. Methods for the measurement of acid aerosol in air are of current interest to individuals engaged in the abatement of air pollution.

This progress report is organized in three sections. The first section deals with the numerical analysis of a set of equations describing the size distribution of an aerosol continuously reinforced by the introduction of particles and undergoing Brownian coagulation. It is believed that this represents the first attempt at the formulation and analysis of this type of an aerosol.

Experimental measurements on the number of acid nuclei formed from the photooxidation of sulfur dioxide in air is presented in Section II. The influence of humidity and initial sulfur dioxide concentration on the number of acid particles formed was investigated.

The third section of this report describes the development of a novel method for the measurement of acid nuclei. The method is an adaptation of the spark replica method used for the detection of nuclear particles.

SECTION I

Coagulation of a Continuously Reinforced Aerosol

GENERAL

The particle size distribution of an aerosol is influenced by coagulation, sedimentation, the rate of generation of particles, particle characteristics and the dynamics of the fluid in which the particles are suspended. The air pollution specialist is interested in the description of particle concentrations and size distribution and in how they are dependent on the physical and chemical processes occurring in the urban atmosphere. If a sufficiently complete description of the atmospheric aerosol and its dynamic behavior were available, the prediction of time and spatial variation of aerosol concentration would be possible. The interrelationship of aerosol concentration and the rate of particle generation (direct emission or formation within the atmosphere) could be established. For this investigation, the changes in the particle size distribution of a coagulating, non-sedimenting aerosol continuously reinforced with particles are described.

The particle size distribution of an aerosol continually reinforced by the introduction of particles (feed) and undergoing Brownian coagulation was calculated by numerically integrating the equations of Smoluchowski modified to include a feed term. A variation of the Adams' method of integration was used. The usefulness of the rather simple aerosol model lies in the possibility of extracting qualitative information on the dependence of particle size distribution and concentrations on particle feed rate and feed characteristics. The influence of heterogeneity on the coagulation process itself was examined also.

Concentrations for different size particles as a function of time were computed for different functional representations of particle feed and coagulation coefficient. The influences of these factors on the resulting equilibrium size distribution were examined. The functional form of the diffusion coefficient used in the calculations is applicable to the diffusive coagulation regime and not to the gas-kinetic coagulation regime (1). This limitation restricts the applicability of the calculations to Knudsen number less than one or to a lower limit of particle size > 0.05 micron radius in air.

Hidy (2) has computed numerically the size distribution of an aerosol, using the discrete equations of Smoluchowski. The approaches used by Hidy (2) and in the work reported here are basically similar. The major difference between the aerosol considered by Hidy (2) and the aerosol model considered here is as follows. Hidy (2) considered the concentration decrease of an initially specified aerosol of constant mass. This investigation concerns itself with the changes in the size distribution of an aerosol continuously reinforced with particles. The mass of this aerosol was zero initially and increases linearly with time.

The physical situations giving rise to the two types of aerosol are also different. For the aerosol model presented, the particle generation term in the equations was intended to represent the physical processes of direct particle emission into the atmosphere or of particle formation in the atmosphere by chemical reactions, e.g., the photochemical reaction of unsaturated hydrocarbons and oxides of nitrogen.

General Equations

The Smoluchowski (1918) theory of coagulation, adapted for an input of particles, is expressed by the family of first order non-linear differential equations

$$\frac{d}{dt}(n_k) = F_k + \frac{1}{2}\sum_{i+j=k} 4\pi D_{ij} R_{ij} n_i n_j - \sum_{j=1}^{\infty} 4\pi D_{jk} R_{jk} n_j n_k \quad , \tag{1}$$

$$k = 1,2,3,\ldots,\infty,$$

where i, j and k are positive integers; and

n_k = number concentration of particles of size k,

t = time,

D_{ij} = relative diffusion coefficient characteristic of i and j particles each exhibiting Brownian motion, $(D_i + D_j)$,

R_{ij} = radius of the sphere of influence for an i and a j particle undergoing coagulation, $(r_i + r_j)$,

$2r$ = twice the physical radius of a particle, proportional to $k^{1/3}$,

and

F_k = rate of input of particles of size k.

The left side of Eqs. (1) is the change of particle concentration of size k with time. The first term on the right side is the particle feed rate of size k, the second term represents the rate of formation of particles of size k due to coagulation of particles smaller than size k, and the third term represents the rate of loss of particles of size k due to the coagulation of k size particles with particles of every size.

The initial conditions for the system considered in this work are $n_k = 0$ at $t = 0$, $k = 1,2,\ldots,\infty$. Eqs. (1) may be non-dimensionalized by dividing each term by $\frac{2kT}{3\mu} N^2$, in which k is Boltzmann's constant, T is the absolute temperature, μ, is the absolute viscosity of the medium, and N is the total concentration of particles at $\tau = \infty$. The non-dimensionalized expression is

$$\frac{d\nu_k}{d\tau} = I_k + \sum_{i+j=k} K_{ij}\nu_i\nu_j - 2\nu_k \sum_{j=1}^{\infty} K_{kj}\nu_j \quad , \qquad (2)$$

$$k = 1,2,3,. \ . \ . \ . \ \infty,$$

where

$$\nu_k = \frac{n_k}{N} \ ,$$

$$\tau = \frac{2kT}{3\mu} N \ t,$$

$$K_{ij} = \frac{D_{ij}R_{ij}}{kT/3\pi\mu} \ ,$$

and

$$I_k = \frac{3\mu F_k}{2kTN^2} \ .$$

The time dependent particle size distribution for the entire system can be determined, in principle, from this family of equations. The behavior of systems with a constant rate of input of unit size particles and of particles distributed with respect to size was studied for two representations of the coagulation coefficient. A constant coagulation coefficient and a coagulation coefficient dependent on the sizes of the colliding particles were used in the computations.

Other than the case of constant coagulation coefficient , the coagulation coefficients were written as functions of the interacting particle sizes. The size dependency of the coagulation rate constant was computed from the Stokes-Einstein relation for the diffusion constant, the Cunningham correction factor, and the experimental observations of Millikan (3). The expression utilized is

$$K_{ij} = \frac{1}{4}\left\{\left[2 + \frac{r_j}{r_i} + \frac{r_i}{r_j}\right] + S\left(\frac{r_1}{r_i}\right)\left(1 + \frac{r_j}{r_i}\right)\left[A + B\exp\left(-\frac{C}{S}\frac{r_j}{r_1}\right)\right] + S\left(\frac{r_1}{r_j}\right)\left(1 + \frac{r_i}{r_j}\right)\left[A + B\exp\left(-\frac{C}{S}\frac{r_i}{r_1}\right)\right]\right\} \quad (3)$$

where $S = \frac{\lambda}{r_1}$. In this expression, λ is the molecular mean free path of the gas medium, A = 0.864, B = 0.290, and C = 1.25. The effect of a variable K_{ij} was studied by using K_{ij} = constant and using Eq. (3) with S = 0, 0.5, 1, and 5.

The expressions used for the feed term are

$$I_1 = 1$$

$$I_k = 0 \qquad k = (2,3,\ldots,\infty)$$

for an input of unit size particles only and

$$I_k = \frac{1}{\sqrt{2\pi}\, k \ln \sigma_k} \exp\left[-\frac{1}{2}\left(\frac{\ln k/k_o}{\ln \sigma_k}\right)^2\right], \quad (4)$$

$$k = 1,2,3,\ldots,\infty,$$

where σ_k and k_o are parameters of the distribution.

Mathematical Solution for the Case with Constant Coagulation Coefficient

Since the equations are non-linear, most of the following solutions were obtained numerically. Some information, however, can be obtained for the one simplified case of constant coagulation coefficient. Thus, if $K_{ij} = K_{11}$, the equations reduce to

$$\frac{d\nu_k}{d\tau} = I_k + K_{11} \sum_{i+j=k} \nu_i \nu_j - 2\nu_k K_{11} \sum_{j=1}^{\infty} \nu_j \quad , \tag{5}$$

$$k = 1,2,3,. \; . \; . \; . \; \infty,$$

Adding these equations gives

$$\frac{d}{d\tau}\left(\sum_{k=1}^{\infty} \nu_k\right) = \sum_{k=1}^{\infty} I_k + K_{11} \sum_{i=1}^{\infty} \sum_{j=1}^{\infty} \nu_i \nu_j - 2K_{11} \sum_{k=1}^{\infty} \nu_k \sum_{j=1}^{\infty} \nu_j$$

$$= I_T - K_{11}\left(\sum_{k=1}^{\infty} \nu_k\right)^2 \quad , \tag{6}$$

in which

$$I_T = \sum_{k=1}^{\infty} I_k \quad .$$

This result is a nonlinear differential equation of the Riccatti type, for which solution techniques are available. The solution of this particular equation is

$$\sum_{i=1}^{\infty} \nu_k = (I_T/K_{11})^{\frac{1}{2}} \tanh\left[(I_T K_{11})^{\frac{1}{2}} \tau\right] \tag{7}$$

The time dependent concentration for the unit size particle can also be determined in closed form. Thus,

$$\frac{d\nu_1}{d\tau} = I_1 - 2(I_T K_{11})^{\frac{1}{2}} \nu_1 \tanh\left[(I_T K_{11})^{\frac{1}{2}}\tau\right] \tag{8}$$

has the solution

$$\nu_1 = \frac{1}{2}\left[\frac{I_T}{K_{11}}\right]^{\frac{1}{2}}\left[\frac{I_1}{I_T}\right]\left[\frac{\sinh 2(I_T K_{11})^{\frac{1}{2}}\tau + 2(I_T K_{11})^{\frac{1}{2}}\tau}{\cosh 2(I_T K_{11})^{\frac{1}{2}}\tau + 1}\right] . \tag{9}$$

The solutions to the differential equations for all other size particles are unwieldly for analytical techniques and were obtained using numerical integration techniques.

Numerical Techniques

Solutions to the general problem with variable coagulation coefficients, as well as the remaining portions of the constant coagulation coefficient case, were studied using a variation of the Adams' numerical method for solving ordinary differential equations. A Runge Kutta method was used for starting the solution i.e., the first three time steps. Values of 0.2, 0.1 and 0.05 were utilized for $\Delta\tau$, with $\Delta\tau = 0.2$ being satisfactory for many cases. For values of $(\lambda/r_1) = 1$, time steps of 0.05 was necessary for avoiding oscillations in the calculated values of concentration. The numerical work utilized the one hundred equations representing the coagulation of the unit size particle and multiples of it up to particles whose volume is 100 times that of the unit particle. The computer program was written with subroutines for the coagulation coefficients and for the input distribution.

RESULTS AND DISCUSSION

Particle concentrations of size k and the total particle concentration as a function of time are shown in Fig. 1 for a constant rate of input of unit size particles and for three different coagulation coefficients. The concentration and time are dimensionaless parameters as defined by Eqs. (2). The size parameter k is the number of unit size particles in an agglomerate. The concentration of any particular size, ν_k, overshoots its equilibrium value during its approach to equilibrium. The total rate of input was one, i.e., $I_T = I_1 = 1$. The results obtained can be scaled for other values of I_T. The concentrations are proportional to $(I_T)^{\frac{1}{2}}$ and the times are inversely proportional to I_T. The total particle concentration increases monotonically. In comparing the concentrations obtained with a constant coagulation coefficient with the results obtained for coagulation coefficients dependent on the sizes of the colliding particles, it is seen that both the magnitude of the peak concentration and the time associated with it are less for the latter cases. The smaller values of τ for the peak concentration reflect an acceleration of the coagulation process. The lower values of the peak concentration, however, do not reflect a damping of the peak concentrations in relation to their equilibrium values. The ratio of peak to equilibrium values for the cases presented in Fig. 1 are all about 1.8.

Results obtained for a constant coagulation coefficient and an input of particles distributed with respect to size in accordance with Eq. (4) are shown in Fig. 2. For this computation, $I_T = 1$, $k_o = 10$, and $\sigma_k = 2.5$. The maximum rate of input is of particles consisting of 4 unit size particles. The relative rates of I_4, I_{10}, and I_{50} are 0.0664, 0.0440, and 0.0018. The approach toward equilibrium, for a given particle size, follows a similar pattern as that shown in Fig. 1.

The dependence of the coagulation coefficient on the sizes of the colliding particles accelerates the coagulation process and decreases the time necessary to reach equilibrium. The differences in the size distributions obtained with a constant coagulation coefficient and with

a size dependent coagulation coefficient are negligible for $(\lambda/r_1) = 0$; and not particularly pronounced for $(\lambda/r_1) = 1$. The effect of introducing particles distributed with respect to size is also to accelerate the approach toward an equilibrium size distribution. The equilibrium concentration of a particular particle size and the amount of overshoot are reduced by the early appearance of larger particles.

Fig. 3 indicates how the concentration-size curve changes with time for a coagulation coefficient of one, $K_{ij} = 1$, and a constant rate of input of unit size particles, $I_1 = 1$. At any one value of τ, the concentrations of small-size particles are but slightly greater than their equilibrium values. Concentrations of the larger particles are considerably less than their equilibrium values. The decrease in concentration with size is quite marked. At larger values of τ, the character of the concentration-size curve is unchanged, but the marked decrease in concentration is associated with progressively larger particle sizes. Equilibrium concentrations are thus not attained simultaneously for all particle sizes. The small-size particles reach equilibrium concentrations relatively rapidly, at τ values of approximately two for unit size particles. The concentration of particles consisting of 100 unit size particles approaches its equilibrium value at τ much greater than 10, although the concentration at $\tau = 10$ is numerically close to the equilibrium value. The equilibrium size distribution for this case is described (4) by the power expression $(\nu_k/\nu_2) = 2^{3/2}\, k^{-3/2}$.

The size distribution is shown on a semi-log plot in Fig. 4 for a constant coagulation coefficient and a feed of particles distributed with respect to size. The feature illustrated is the constant size associated with peak concentrations at different times. For a coagulating aerosol with feed, the maximum in the size distribution curve reflects a characteristic of the particle density function (Eq. (4)); this maximum shifts only slightly with time. Hence, the peak size of an aerosol at any time gives information on the peak size of particles being continuously introduced. This invariant property can be used as a check on the applicability of the aerosol model to experimental systems such as photolysis of hydro-

carbons resulting in the formation of particles. The slowness of the larger particles in attaining equilibrium values as contrasted with the peak size is evident. The constant peak size is a property of an aerosol continuously reinforced with particles and may be used to distinguish it from the initially constant mass, decaying aerosol discussed by Hidy (2). The peak size of an aerosol without reinforcement shifts to an ever larger size with increasing time.

The influence of size dependency of the coagulation coefficient on the equilibrium concentration and time necessary to attain this value for a given particle size is shown in Fig. 5. As with the constant rate of input of unit size particles, the difference in the concentration-size curve, for any given value of τ, between a constant coagulation coefficient and a size dependent coefficient with $(\lambda/r_1) = 0$ is small. Comparison of results for $(\lambda/r_1) = 0$ and $(\lambda/r_1) = 1$ in Fig. 5 indicates that the greater size dependency of the coagulation coefficient results in a higher concentration of large size particles in the early stages, but a lower equilibrium concentration is finally attained. The first 100 particle sizes are essentially at equilibrium at $\tau = 4$. Thus, the size dependency of the coagulation coefficient has a relatively minor effect on the aerosol history.

Equilibrium is promoted more by changes in the characteristics of the input aerosol than by the size dependency of the coagulation coefficient. The time to reach equilibrium for any particle size k is approximated by the empirical relation $\tau = Ak + B$. The values of A and B are 0.65 and 2.0 for $K_{ij} = 1$ and $I_1 = 1$; 0.45 and 2.0 for K_{ij}, $(\lambda/r_1) = 1$, and $I_1 = 1$; and 0.02 and 3.0 for K_{ij} and I_k.

The effect of the size dependency of the coagulation coefficient on the coagulation process for the case of constant rate of input of unit size particles is shown in Fig. 6. The variation of concentration as a function of size is for several values of time. The shapes of these curves are similar to those illustrated in Fig. 3. For a given value of τ, the sharp decrease in concentration occurs at a smaller

particle size for $(\lambda/r_1) = 0$ than for $(\lambda/r_1) = 1$. A broader range of particle sizes is formed with the larger value of (λ/r_1). At any given time, the mass of the aerosol is fixed and a wider spectrum of sizes results in a lower concentration. For example, the equilibrium concentration ν_{10} is 0.07 and 0.09 for (λ/r_1) equal one and zero, respectively.

The set of equations, Eqs. (1), used for this investigation was truncated at k = 100. By truncation, one ignores the particles whose size is greater than 100 and the mass associated with these particles. In the aerosol model considered, particles (mass) are continually added to the system. When the concentrations of the first 100 particle sizes approach their equilibrium values, as indicated by the calculations, then the mass associated with particles from k = 1 to k = 100 approaches a constant value. The question as to whether the calculated concentrations converge to the correct values is discussed below.

The accuracy of the computations for ν_k depends on the accuracy of the last summation term in Eqs. (2). The additional requirement that the mass present in the particle size interval for k = 1 to k = 100 be equal to the mass introduced into the system is met, in general, for τ values less than two. This additional requirement, however, is not necessary for the validity of the calculated values of ν_k. For the case of a constant coagulation coefficient and a feed of unit size particles, i.e., $K_{ij} = 1$ and $I_1 = 1$, the numerical results converge to those obtained analytically without meeting the mass balance requirement. The concentration for the unit size particles computed numerically and those computed from the analytic solutions differed by a few parts in ten thousand. Concentrations computed with 50 and 100 equations were substantially the same. Table I shows comparative concentrations obtained with the analytic solutions and those obtained with 50 and 100 equations for time steps of 0.05, 0.1 and 0.2. The use of k = 100 for the upper limit of the summation introduced a maximum error of 0.3%. By truncation, one sacrifices information for particle sizes $k > 100$ but the computations for $k < 100$ are valid.

For the case of a size dependent coagulation coefficient and a feed of unit size particles, the error is of the same order of magnitude as the above case. For the case of an input of particles distributed with respect to size, the computations are accurate for τ values of approximately two and less. This is based on the stringent and unnecessary criterion of mass balance. For the example K_{ij}, I_k, and $(\lambda/r_1) = 0$, the mass in the system for $1 \leq k \leq 100$ is 23.3 at $\tau = 2$ and converges to 26.1 for large values of τ. For $\tau = 2$, the total mass introduced into the system was 28.8. For $\tau > 2$, the difference between the mass in the size interval $1 \leq k \leq 100$ and the total mass introduced into the system thus becomes progressively greater. As discussed previously, this does not imply necessarily that the computations are inaccurate. The accuracy of the computations is much greater than that indicated by the mass balance since the computational error depends on the number of particles omitted by truncation rather than on the mass lost.

REFERENCES

1. Fuchs, N.A. and Sutugin, A.G., "Coagulation Rate of Highly Dispersed Aerosols," J. Colloid Sci., 20, 492-500 (1965).

2. Hidy, G.M., "On the Theory of the Coagulation of Noninteracting Particles in Brownian Motion," J. Colloid Sci., 20, 123-144 (1965).

3. Millikan, R.A., "General Law of Fall of a Small Spherical Body Through a Gas," Phys. Rev., 22, 1-23 (1923).

4. Quon, J.E. and Mockros, L.F., "The Equilibrium Size Distribution of an Aerosol Continuously Reinforced with Particles," Int. J. Air and Wat. Poll., 9, 279-290 (1965).

NOTATIONS

D_{ij} = relative diffusion coefficient characteristic of i and j particles each exhibiting Brownran motion, $(D_i + D_j)$,

F_k = rate of input of particles of size k,

I_k = non-dimensionalized feed rate of particles of size k, $3\mu F_k/2kTN^2$,

I_T = non-dimensionalized total feed rate,

K_{ij} = non-dimensionalized coagulation coefficient, $3\pi\mu D_{ij} R_{ij}/kT$,

k = Boltzmann's constant; number of unit size particles in an agglomerate,

N = reference total concentration of particles, at $\tau = \infty$,

n_k = number concentration of particles of size k,

κ = 2r, twice the physical radius of a particle,

R_{ij} = radius of the sphere of influence for an i and a j particle undergoing coagulation, $(r_i + r_j)$,

r = physical radius of a particle, proportional to $k^{1/3}$,

S = (λ/r_1), slip factor,

T = absolute temperature of gas medium,

t = time,

λ = mean free path of molecules of the medium in which particles are suspended,

μ = viscosity of gas medium,

ν_k = relative particle concentration, n_k/N,

σ_k = geometric standard deviation of particle size, and

τ = non-dimensionalized time, $2kTNt/3\mu$.

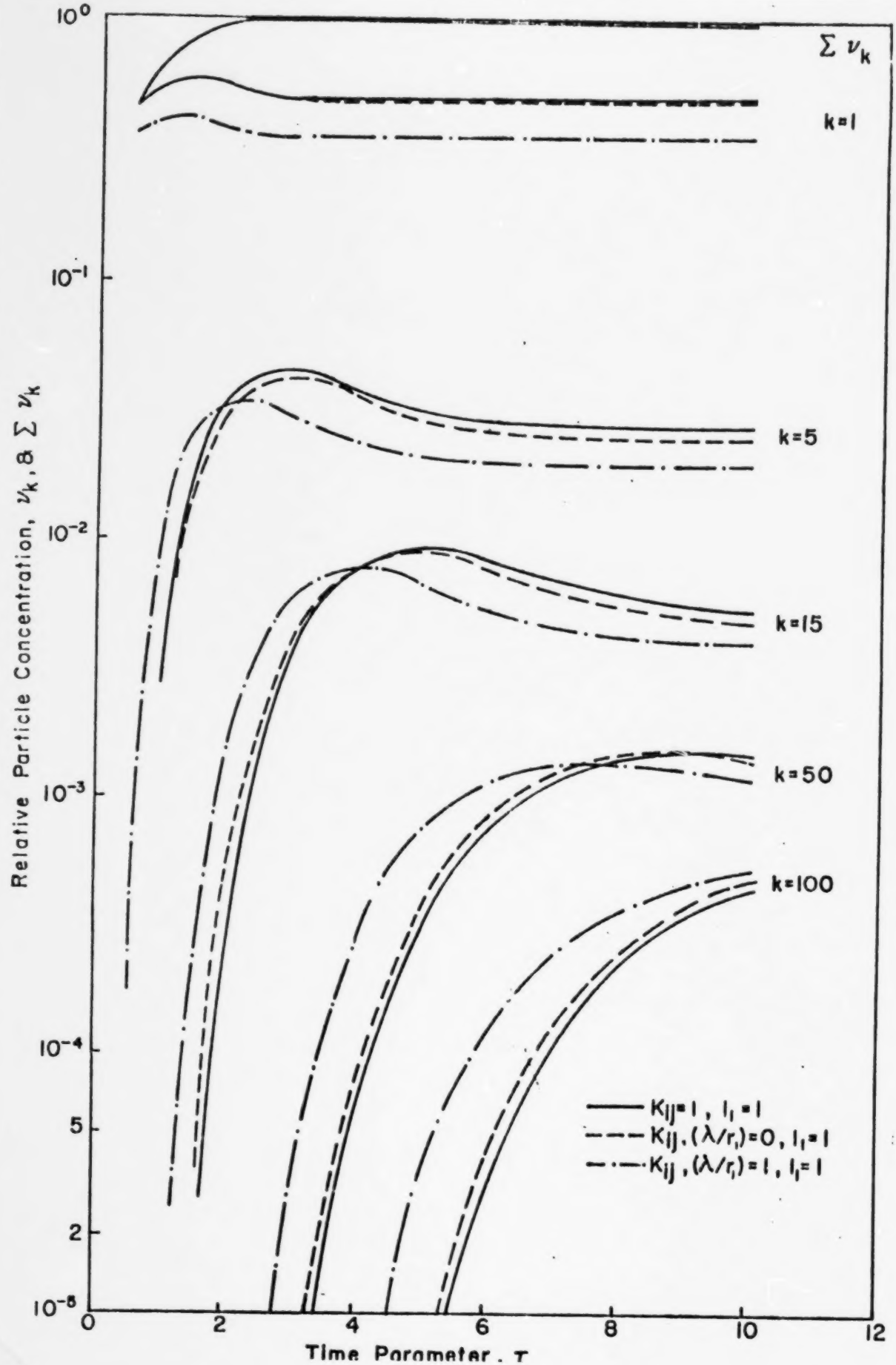

Fig. 1 Particle Concentration as a Function of Time and Size Parameters: $K_{ij} = 1$, $I_1 = 1$; K_{ij}, $(\lambda/r_i) = 0$, $I_1 = 1$; K_{ij}, $(\lambda/r_i) = 1$, $I_1 = 1$.

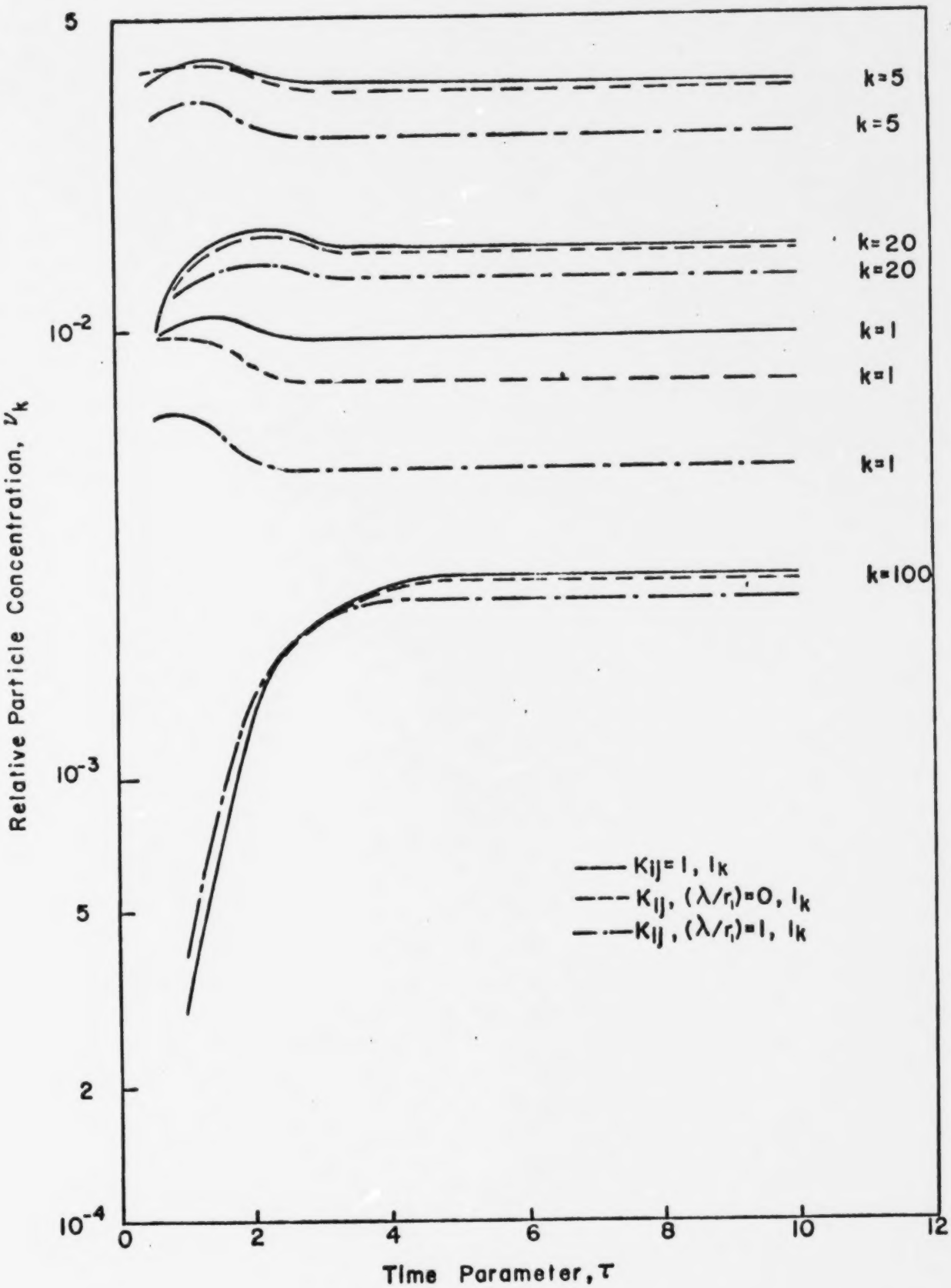

Fig. 2 Particle Concentration as a Function of Time and Size Parameters: $K_{i,j}$, $(\lambda/r_i) = 0$, $I_{i,j}$; $K_{i,j}$, $(\lambda/r_i) = 1$, $I_{i,j}$.

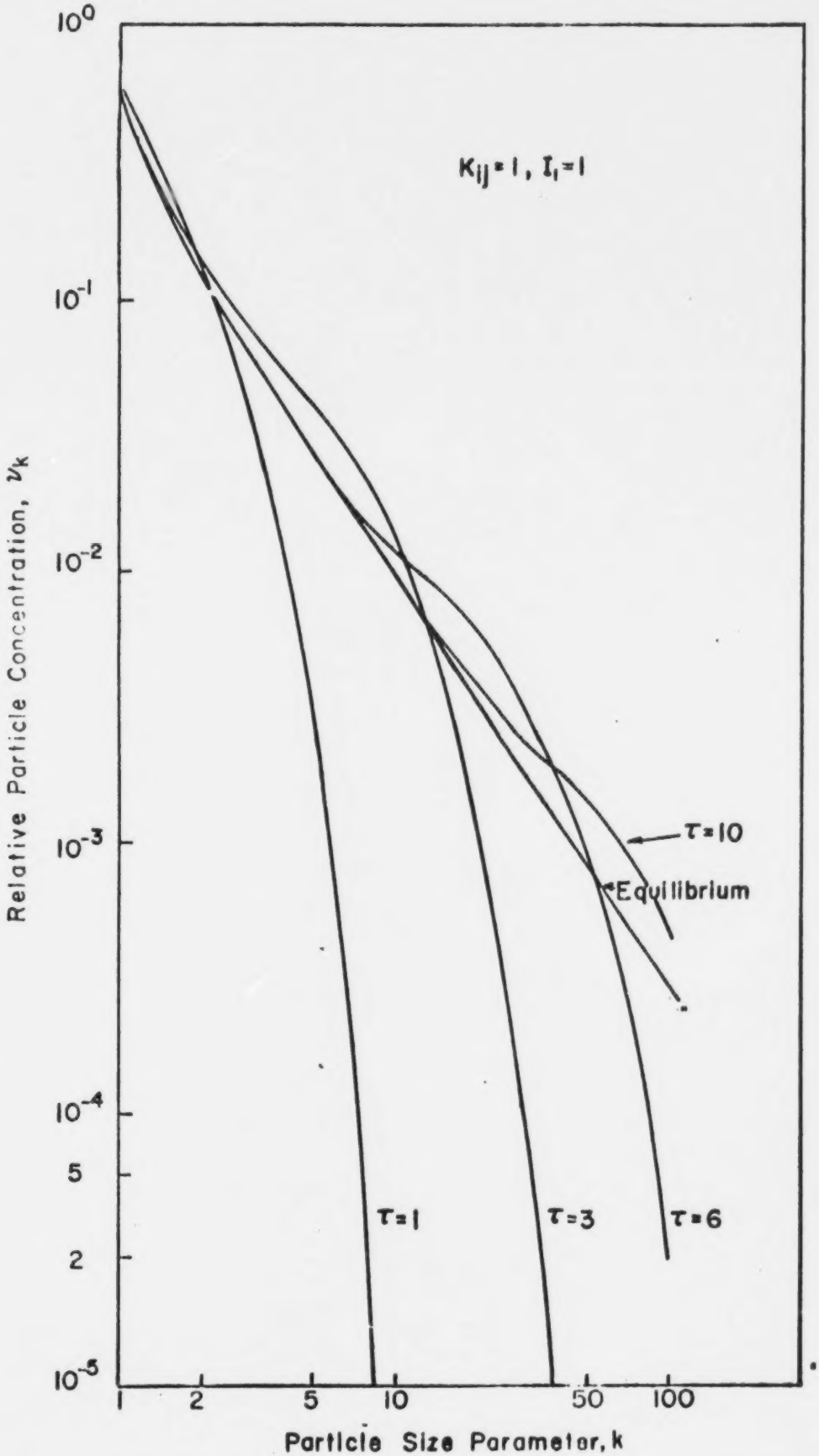

Fig. 6 Particle Concentration versus Size for Different Values of the Time Parameter τ: K_{ij}, $(\lambda/r_j) = 0$, $I_1 = 1$; K_{ij}, $(\lambda/r_j) = 1$, $I_1 = 1$.

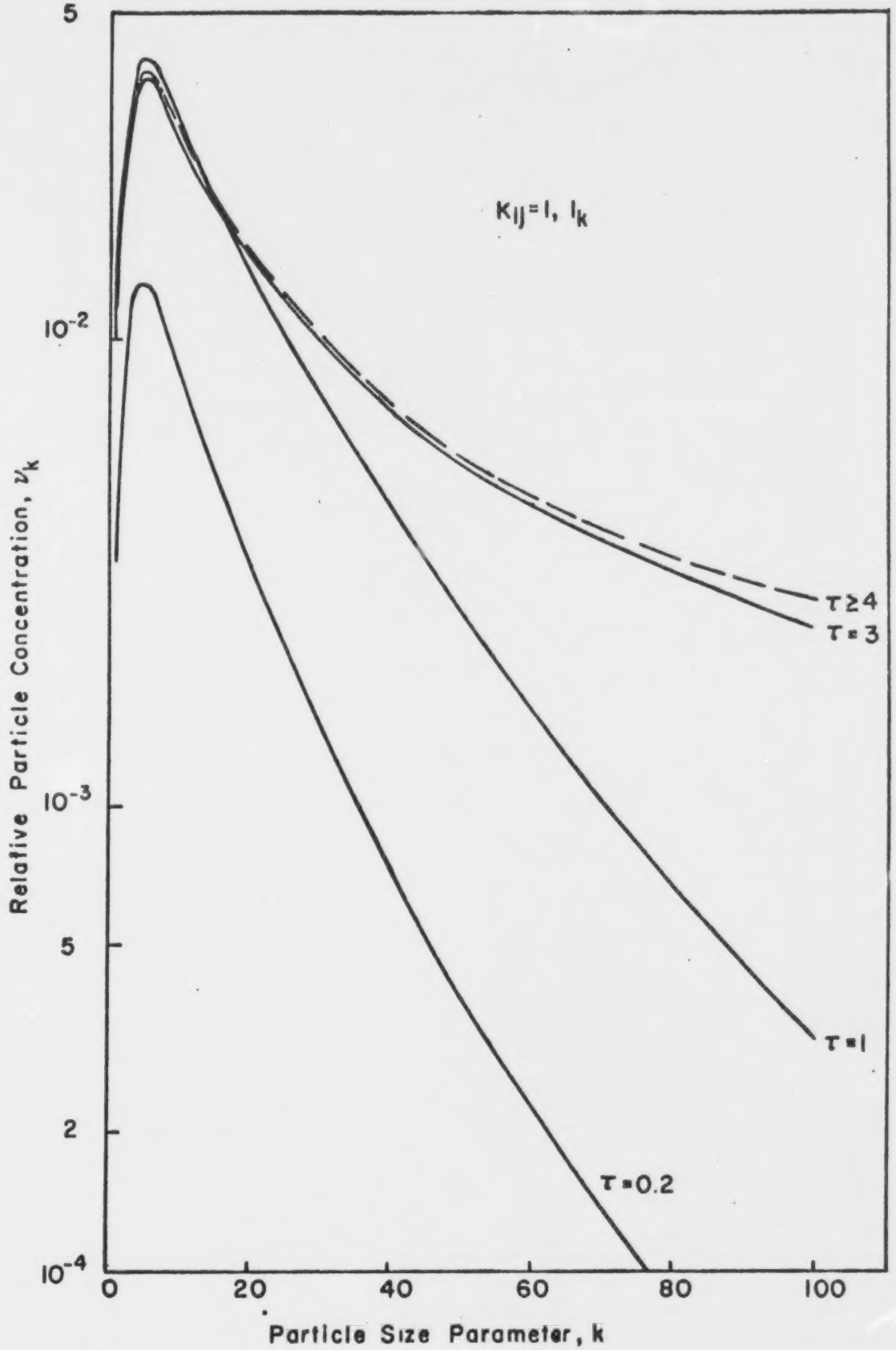

Fig. 4 Particle Concentration versus Size for Different Values of the Time Parameter τ: $K_{ij} = 1$ and I_k.

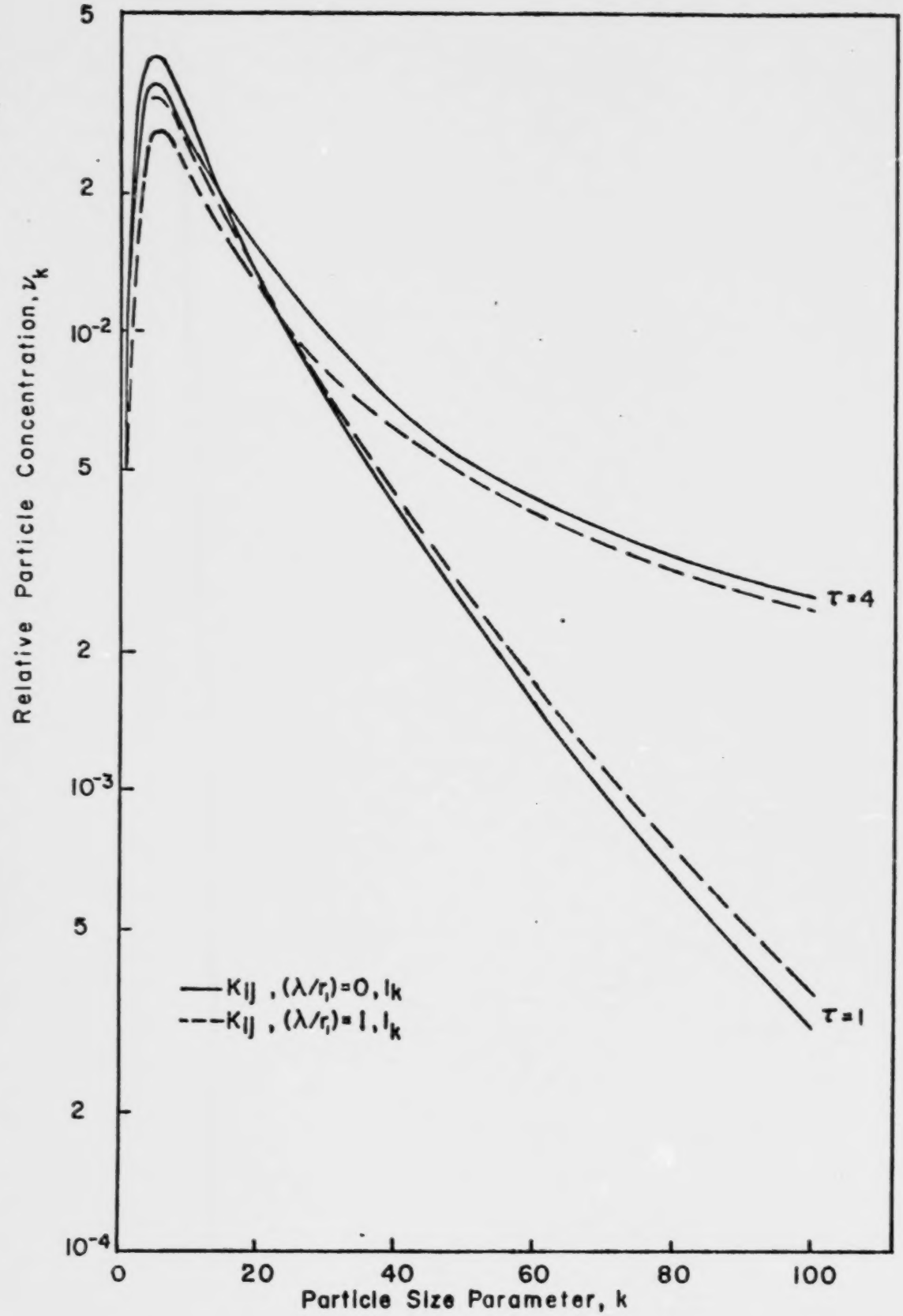

Fig. 5 Particle Concentration versus Size for different Values of the Time Parameter τ: K_{ij}, $(\lambda/r_i) = 0$, I_k; K_{ij}, $(\lambda/r_i) = 1$, I_k.

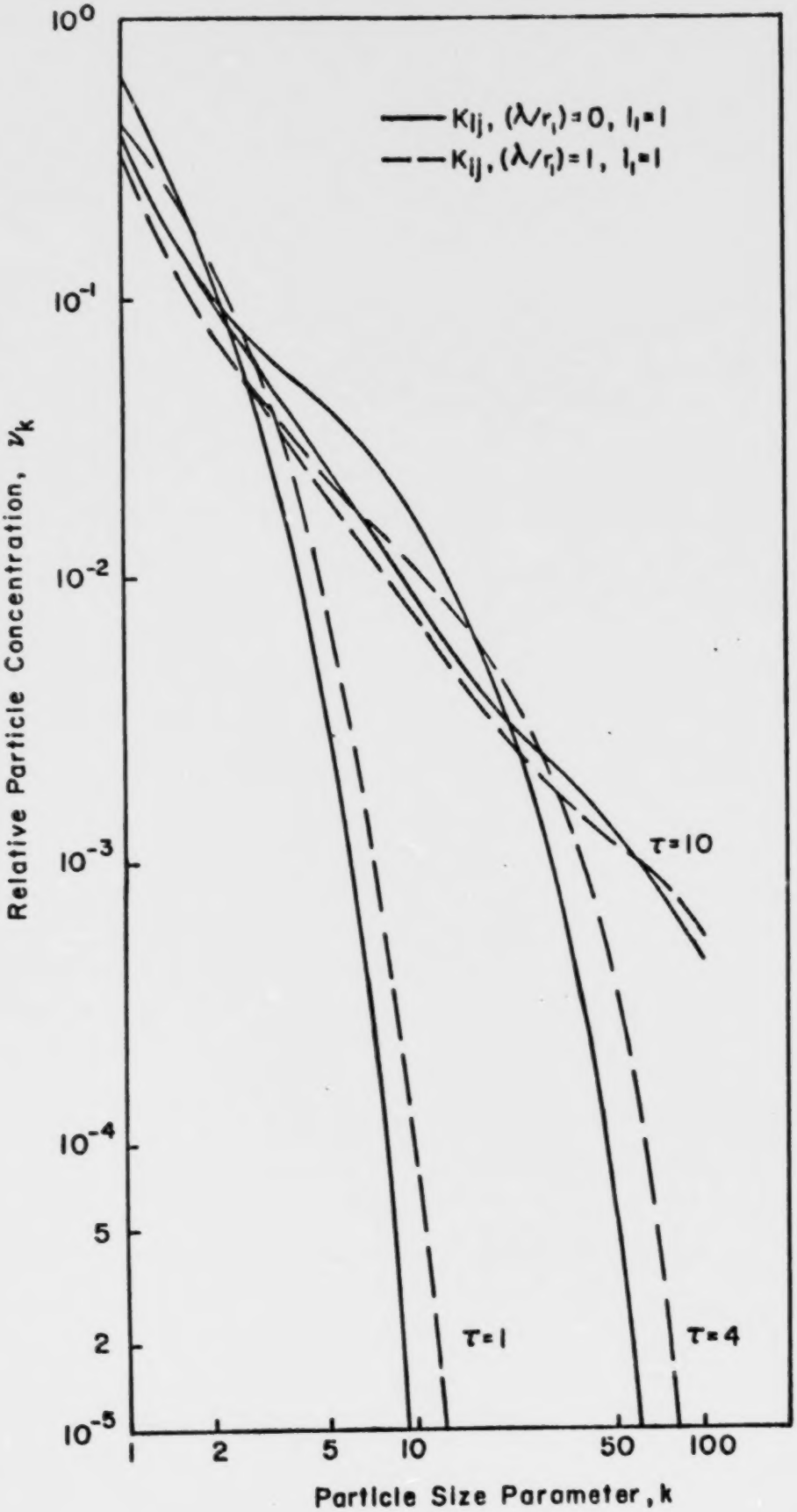

Fig. 3 Particle Concentration versus Size for Different Values of the Time Parameter τ: $K_{ij} = 1$ and $l_i = 1$.

Table 1. Comparison of Numerical Computations with Analytical Solution

($K_{11} = 1$, $I_1 = 1$, $\tau = 3.0$)

Time Step $\Delta\tau$	Relative Particle Concentration					
	50 Eqs.		100 Eqs.		Analytical Solution	
	ν_1	$\Sigma\nu_k$	ν_1	$\Sigma\nu_k$	ν_1	$\Sigma\nu_k$
0.05	-	-	0.5123	0.9950	0.5036	0.9950
0.10	-	-	0.5123	0.9950		
0.20	0.5124	0.9951	0.5124	0.9951		

SECTION II

Particle Formation From Photooxidation of Sulfur Dioxide in Air

GENERAL

Photochemical reactions of sulfur dioxide in air, of oxides of nitrogen-hydrocarbon mixtures in air, and of mixtures of sulfur dioxide, nitric oxide or nitrogen dioxide, and hydrocarbons in air lead to the formation of particulates. The work of Doyle, Schuck, and Renzetti[1-4] demonstrates that sulfur dioxide plays a large part in the photochemical formation of aerosols in polluted air. It has been reported that the presence of sulfur dioxide is essential for the formation of an aerosol from photooxidation of certain unsaturated hydrocarbons and nitric oxides in air[2,5,6]. The photooxidation of sulfur dioxide to sulfur trioxide and subsequent hydration to sulfuric acid may be a significant source of condensation centers for the accumulation of photochemical reaction products and formation of particulates in the size range effective in reducing visibility.

Since the concentration of condensation centers or nuclei resulting from the photooxidation of sulfur dioxide in air is extremely

high, in the order of 10^5 to 10^6 nuclei per cm^3, and the removal of these nuclei by the lung in the course of breathing is also high, health implications of nuclei production in the ambient urban air deserve the attention of investigators concerned with the health aspects of air pollution.

The production of copious nuclei requires only the conversion of a few pphm of sulfur dioxide. The implications of this to establishing air quality standards for sulfur dioxide need to be elucidated. The rate of nuclei production, its dependence on external conditions, and the nature of the nuclei are useful in this regard.

This experimental study on the photooxidation of sulfur dioxide in air was designed to obtain information on the formation of nuclei for different initial concentrations of sulfur dioxide and relative humidities. Concentrations of sulfur dioxide used ranged between 0.20 and 0.65 ppm. Relative humidity was varied between 13 and 77%. The ultraviolet radiation flux of approximately 2500 μ watts/cm^2 in the middle of the batch reaction vessel was supplied by blacklights. The question as to whether the hydrated oxidation product is gaseous or particulate was explored by measuring the nuclei concentration of the irradiated gas mixture before and after filtration through several types of filter media. Some estimates of size and molecules per nuclei were inferred from the data.

EXPERIMENTAL APPARATUS AND PROCEDURES

The formation of particles from irradiation of sulfur dioxide in air was measured for different combinations of initial sulfur dioxide concentrations, relative humidity, and irradiation time. The range of initial sulfur dioxide concentration used was 0.2 to 0.65 ppm; relative humidity varied from 13 to 77% for a dry bulb temperature of 23°C; irradiation time ranged between 0 and 4 minutes; and the light intensity of approximately 2500 μ watts/cm^2 was used. The experiments were conducted on a batch basis.

Particles formed by photooxidation of sulfur dioxide in air were measured by a condensation nuclei meter[7]. The instrument is a Wilson cloud chamber type and responds to particles or nuclei in the size range of 1 to 100 mμ radius. Generally, three measurements were made on each sample.

The compressed cylinder air used in preparing different concentrations of sulfur dioxide was passed through charcoal and cotton filters in series prior to humidification. The filters were approximately an inch in diameter and 6 inches in length. This treatment was sufficient to reduce the initial nuclei concentration to less than 400 per cm^3. The nuclei concentration after irradiation in the absence of sulfur dioxide ranged between 100 and 800 per cm^3 with an average of 300 per cm^3.

The sulfur dioxide-air mixtures were prepared by metering a known rate of air flow through an all glass flask containing a sulfur dioxide permeation tube[8]. The diffusion rate of the

permeation tube was determined from weighings taken over a period of a week at daily intervals. The temperature of the permeation tube was kept constant by keeping the flask in a temperature bath regulated to ± 0.1°C. The compressed air used for the preparature was humidified, as necessary, by bubbling the air through a 12-liter flask which was partially filled with water. The degree of humidification was controlled by the flow rate of air. The air passes through a length of copper tube immersed in a constant temperature bath prior to entering the mixing chamber containing the permeation tube. A flow stream of sulfur dioxide in air at a temperature of 23°C and for differing humidities was obtained in this manner. The relative humidity and temperature of the flow stream were measured with a thermistor type psychrometer.

The sulfur dioxide-air mixture was introduced into air sampling bags made of Saran and the samples were irradiated for a predetermined time period. The sampling bags were pre-conditioned to minimize adsorption losses. The treatment consists of filling the sampling bags with the desired sulfur dioxide-air mixture and emptying the contents after a period of 20 to 25 hours.

The volume of the samples used in the irradiation experiments was approximately 14 liters each. In addition to the pre-conditioning treatment, the bags were flushed with clean air, filled with the sulfur dioxide mixture to be used, emptied, and finally filled with the sample to be investigated. The initial nuclei concentrations of the samples in the bags were generally less than 400 per cm^3 prior to irradiation. In addition to

checking the nuclei concentration of the air used for preparing sulfur dioxide-air mixtures before and after irradiation in the absence of sulfur dioxide, nuclei measurements of the sample prior to irradiation were also made. The transparency of Saran to light at 350 mμ is good, although some deterioration with usage is to be expected[9].

The source of radiation consisted of two parallel banks of GE Blacklights (F20T12-BLB) with a centerline separation of 9 inches. Each bank contained four 20 watt bulbs, 22.5 inches in length and centerline separations of 3 inches. The spectral distribution of the blacklights range from 300 mμ to greater than 400 mμ with a peak at 350 mμ. The intensity of the radiation was measured with a uv meter with a long wave sensor cell. The spectral response of the cell approximates the spectral emission of the blacklights. The spectral response of the cell is somewhat broader with a peak at 360 mμ. The intensity in the middle of the irradiation chamber was 2500 μ watts per cm^2. This takes into account the radiation from both banks of light and shielding by one layer of Saran.

The question of whether the response of the condensation nuclei meter to the irradiated samples was a response to gaseous sulfur trioxide or to nuclei of sulfuric acid was explored. Measurements of nuclei before and after filtration of the irradiated samples through various media were made. Types of filtration media used were Whatman filter paper Nos. 1, 5, and 40; Millipore filter type HA (0.45 μ); molecular sieves, types 5A and 13X (1/16 inch pellets);

and charcoal (12 x 30 mesh). Filters of granular material were approximately 1 inch in diameter and 1/4 inch in thickness.

In addition to the filtration experiments, the loss of nuclei through 2 to 10 foot lengths of 1/4 inch tygon tubing, and through two foot lengths of tubing wetted with 1 N NaOH solution or coated with 1 N NaOH solution and dried, was measured. These measurements can serve to distinguish between losses by molecular diffusion and diffusion of small particles to the walls of the tubes.

RESULTS AND DISCUSSION

The photooxidation of sulfur dioxide in air yields sulfur trioxide. The sulfur trioxide is subsequently hydrated in the presence of moisture and forms sulfuric acid. The rate of photooxidation has been determined by Hall[10], Gerhard and Johnstone[11], and Renzetti and Doyle[1]. The reaction is first order with respect to sulfur dioxide. Quantum yield for the reaction reported ranges from 3×10^{-3} to 0.3 with corresponding overall reaction rate constants of 10^{-3} per hour to 4.5×10^{-3} per minute. The reasons for these large variations are not apparent. Differences in spectral characteristics of radiation used and its intensity may account for part of the variations. The rate of reaction may be highly dependent on the concentrations of sulfur dioxide and sulfur trioxide or initial nuclei concentration.

For weak absorption and a first order reaction,

$$\frac{d(SO_3)}{dt} = k_1(SO_2) = \Phi\, k_a(SO_2) \qquad (1)$$

where k_1 = the reaction rate constant,

k_a = the specific absorption rate, and

Φ = the quantum yield.

Integrating Eq. (1),

$$(SO_3) = (SO_2)_o\,(1 - e^{-k_1 t}) \simeq (H_2SO_4) \qquad (2)$$

where $(SO_2)_o$ = the initial concentration of sulfur dioxide, and

t = irradiation time.

The nuclei measurements do not give a direct measurement of the initial product of oxidation, SO_3, nor of H_2SO_4. Doyle[12] has adapted the usual model for the embryo to calculate the self-nucleation rate for the sulfuric acid-water system. In elementary one component systems, the concentration of embryos or nuclei is related to the degree of supersaturation[13]:

$$\ell n\, n = g\, \ell n\, S - \frac{4\pi r^2 \sigma}{kT} + \ell n\, n_o \qquad (3)$$

where n = number of embryos or nuclei,

n_o = number of molecules in a system,

g = number of molecules in an embryo or nucleus,

S = ratio of vapor pressure to equilibrium vapor pressure,

r = radius of embryo,

σ = the specific surface energy of the liquid-vapor interface,

k = Boltzman constant, and

T = absolute temperature.

For a two component system, the relationship is more complicated.

However, Doyle[12] has shown that sulfuric acid partial pressures in the order of one part per hundred billion give rise to rapid self-nucleation; the radii of embryos are in the order of 6 Å; and the corresponding number of molecules per embryo is approximately 20. The value of n is most sensitive to S and the relation of nuclei concentration to sulfuric acid concentration may be represented by

$$\ell n\ n = g\ \ell n\ (H_2SO_4) + A. \tag{4}$$

Combining Eq. (4) with Eq. (2) and rearranging,

$$\ell n\ n = g\ \ell n\ (1-e^{-k_1 t}) + g\ \ell n\ (SO_2)_o + A. \tag{5}$$

The nuclei measurements obtained for different initial sulfur dioxide concentrations, relative humidities, and irradiation times were examined with the aid of Eqs. (2) and (5).

The reaction rate constant, estimated from the average radiation intensity inside the sample bags of 2500 μ watts/cm^2, a quantum yield of 0.3, and a wavelength of 350 mμ, was calculated to be 5×10^{-6}/sec. For small conversions, typical of photooxidation of sulfur dioxide,

$$\ell n\ n = g\ \ell n\ t + B \tag{6}$$

The relationship between n and t is not dependent on an explicit knowledge of k_1 for small conversions. The value of g is expected to be dependent on relative humidity and on the degree of supersaturation with respect to sulfuric acid.

The form of Eq. (4) may also be obtained by treating embryo formation as analogous to polymerization of monomeric molecules.

$$A_1 + A_1 = A_2 \tag{7}$$

$$A_2 + A_1 = A_3 . \tag{8}$$

The subscripts refer to the number of molecules in the polymer. However, if reactions (7) and (8) are much slower than subsequent growth, they nearly reach equilibrium. Writing the rate equations for each species and assuming equilibrium,

$$A_2 = K_1 (A_1)^2 \tag{9}$$

$$A_3 = K_2 (A_2)(A_1) \tag{10}$$

$$A_3 = K_1 K_2 (A_1)^3 \tag{11}$$

In general,

$$A_g = K_1 \ldots . K_{g-1} (A_1)^g \tag{12}$$

and

$$\ell n (A_g) = n \ell n (A_1) + B \tag{13}$$

For a given initial concentration of sulfur dioxide, a log-log plot of nuclei concentration versus irradiation time will give some indication of the value of g, the number of molecules in a nucleus (Eq. (6)). Similarly, if the irradiation time is held constant, a log-log plot of nuclei concentration versus the initial sulfur dioxide concentration will give an estimate of the value of g (Eq. (5)). Nuclei concentrations for irradiation times of 30 to 240 seconds for several ranges of relative humidity and initial sulfur dioxide concentration of 0.20 ppm are tabulated in Tables 1 through 4. The nuclei concentrations tabulated are average concentrations for eight separate experiments. The variation in nuclei concentration for any given period of irradiation is rather large, the standard deviation being in the same order of magnitude as the average. The coefficient of variability is in the order of one. Many sampling bags were used in the study and the variation in the radiation transmission may be 15% from bag to bag due to the variability in the Saran or to aging of the Saran. Eq. (1) indicates that the rate of conversion of sulfur dioxide to the trioxide is proportional to the intensity of radiation.

The relationship between nuclei concentration and irradiation time is shown in Figure 1. The slope of the line indicates a value of 3 for g, the number of molecules pe ucleus. This is in general agreement with the value of 2-20 estimated by Doyle[12] from thermodynamic considerations. A dependence of the relationship shown in Figure 1 to relative humidity is not strong. This is not particularly surprising since the concentration of water mole-

cules is very large in comparison with that of sulfur trioxide, even at a relative humidity of 13-19%.

For sulfur dioxide concentrations typical of air pollution episodes (0.65 ppm), nuclei concentrations resulting from photooxidation were extremely high and beyond the sensitive range of the nuclei condensation meter. These high concentrations were estimated by an extrapolation of the concentrations determined at different time intervals after the irradiation period. The time intervals are designated as coagulation time intervals in Table 5. The basis for the extrapolation is as follows. Coagulation and diffusion of nuclei to the walls of the container act simultaneously to decrease the concentration. Initially, when the concentration is high, the decrease in concentration due to coagulation is dominant. At later periods, when the concentration is small, the decrease due to diffusion (wall losses) becomes dominant. For details, consult Quon[14].

The value of g may also be estimated from a log-log plot of nuclei concentration versus the initial sulfur dioxide concentration, as indicated by Eq. (5). Table 6 summarizes the nuclei concentration observed for different initial sulfur dioxide concentrations and an irradiation time of one minute. Figure 2 gives the same information graphically. The value of g, as given by the slope of Figure 2, is 4.75. This is consistent with the value discussed earlier.

Sulfur trioxide undergoes hydration and self-nucleation readily. Whether the response of the condensation nuclei

meter represents a response to gaseous sulfur trioxide, sulfuric acid vapor or to embryos of sulfuric acid molecules (nuclei) needs some clarification. Nuclei meter readings (nuclei concentration) were obtained on irradiated sulfur dioxide-air mixtures before and after filtration through various filtration media (see Table 7) in an attempt to partially resolve this question. It is accepted generally that room air contains small particles. Reductions in nuclei meter readings as shown in Table 7 are very high for both room air nuclei and irradiated sulfur dioxide when various types of filter paper are used. However, the interpretation of these results is inconclusive since a chemical reaction between an acid gas and the filters is possible. The reductions observed for the charcoal and molecular sieve filters may conceivably be attributed to adsorption of the acid vapor by the media.

The reductions in nuclei readings through cylindrical tubing is more difficult to defend on the basis of a gaseous photooxidation product. Diffusion loss of a gaseous product through 2 feet of 1/4 inch tubing may be expected to be greater than 95%. The relatively small losses shown in Table 8 for the 2 foot tygon tube and for rubber tubes with an inside coating of sodium hydroxide is evidence that substantial numbers of nuclei are formed on irradiation of sulfur dioxide. The magnitudes of losses for various lengths of tubes suggest that the radii of the nuclei are in the order of $10\,\text{Å}$.[15]

REFERENCES

1. Renzetti, N.A. and Doyle, G.J., "Photochemical Aerosol Formation in Sulfur Dioxide-Hydrocarbon Systems," Int. J. Air Poll., 2, 327 (1960).

2. Schuck, E.A., Doyle, G.J., and Endow, N., "A Progress Report on the Photochemistry of Polluted Atmospheres," Rept. No. 31, Air Pollution Foundation, San Marino, Calif., 1960.

3. Schuck, E.A. and Doyle, G.J., "Photooxidation of Hydrocarbons in Mixtures Containing Oxides of Nitrogen and Sulfur Dioxide," Rept. No. 29, Air Pollution Foundation, San Marino, Calif., 1959.

4. Schuck, E.A., Ford, H.W., and Stephens, E.R., "Air Pollution Effects of Irradiated Automobile Exhausts as Related to Fuel Composition," Rept. No. 26, Air Pollution Foundation, San Marino, Calif., 1958.

5. Prager, M.J., Stephens, E.R., and Scott, W.E., "Aerosol Formation from Gaseous Air Pollutants," Industr. and Engn. Chem., 52, 521 (1960).

6. Stevenson, H.J.R., Sanderson, D.E., and Altshuller, A.P., "Formation of Photochemical Aerosols," Int. J. Air and Wat. Poll., 9, 367 (1965).

7. Quon, J.E., "A New Method for the Relative Calibration of a Small Particle Counter," Amer. Industr. Hyg. Assn. J., 25, 15 (1964).

8. O'Keefe, A.E. and Ortman, G.C., "Primary Standards for Trace Gas Analysis," Anal. Chem., 38, 760 (1966).

9. Wilson, K.W. and Buchberg, H., "Evaluation of Materials for Controlled Air Reaction Chambers," Industr. and Engn. Chem., 50 (11), 1705 (1958).

10. Hall, T.C., Jr., "Photochemical Studies of Nitrogen Dioxide and Sulfur Dioxide," Doctoral Thesis, University of California at Los Angeles, 1953.

11. Gerhard, E.R. and Johnstone, H.F., "Photochemical Oxidation of Sulfur Dioxide in Air," Industr. and Engn. Chem., 47, 972 (1955).

12. Doyle, G.J., "Self-Nucleation in the Sulfuric Acid-Water System," J. Chem. Phys., 35 (3), 795 (1961).

13. Nielsen, A.E., Kinetics of Precipitation, The MacMillan Co., New York, 1964.

14. Quon, J.E., "Experimental Determination of the Coagulation Rate Constant for Nuclei," Int. J. Air and Wat. Poll., 8, 355 (1964).

15. Fuchs, N.A., The Mechanics of Aerosols. The MacMillan Co., New York, 1964.

LIST OF NOTATION

A = a constant

B = a constant

g = number of molecules in an embryo or nucleus

k = Boltzman constant

K_1, k_1 = reaction rate constants

k_a = the specific absorption rate

n = number of embryos or nuclei

r = radius of embryo

S = ratio of vapor pressure to equilibrium vapor pressure

T = absolute temperature

t = irradiation time

(X) = concentration of component X

σ = the specific surface energy of the liquid-vapor interface

ϕ = the quantum yield

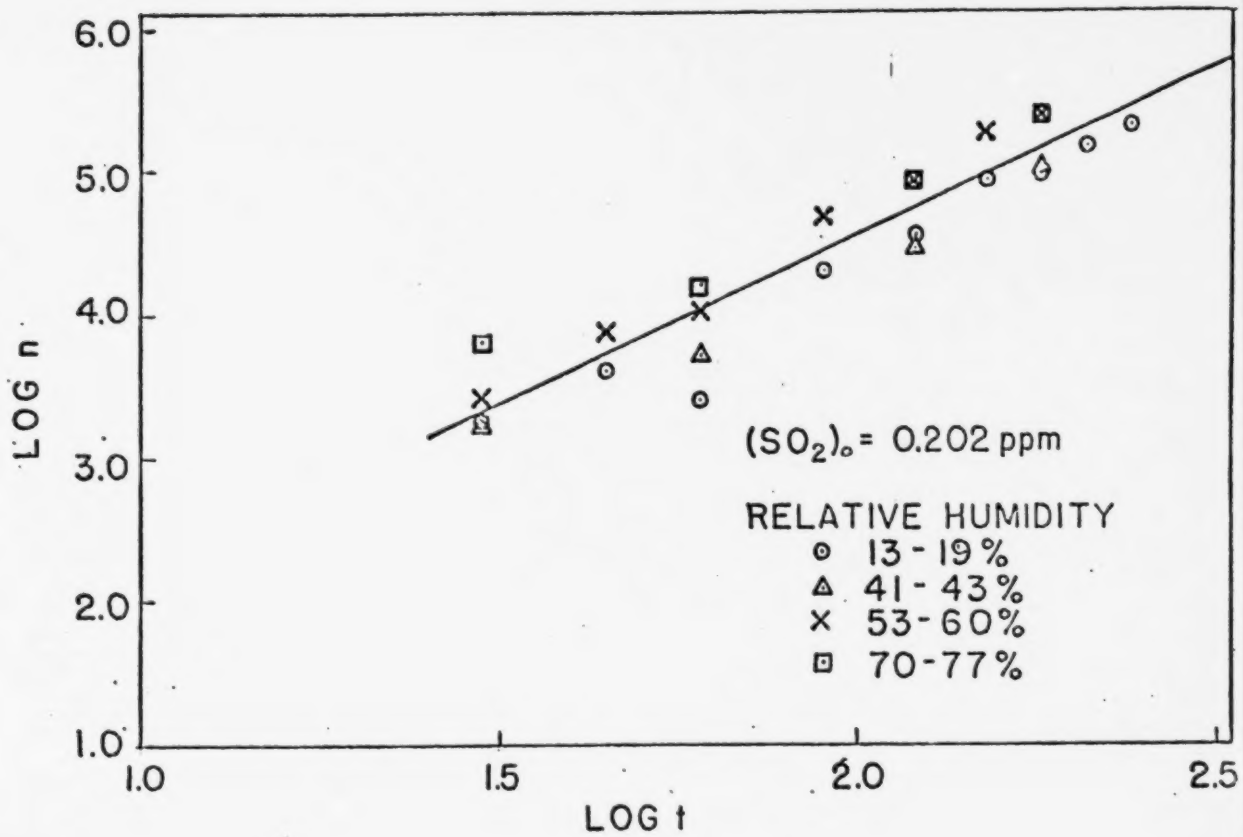

Figure 1. Nuclei Concentration vs Irradiation Time

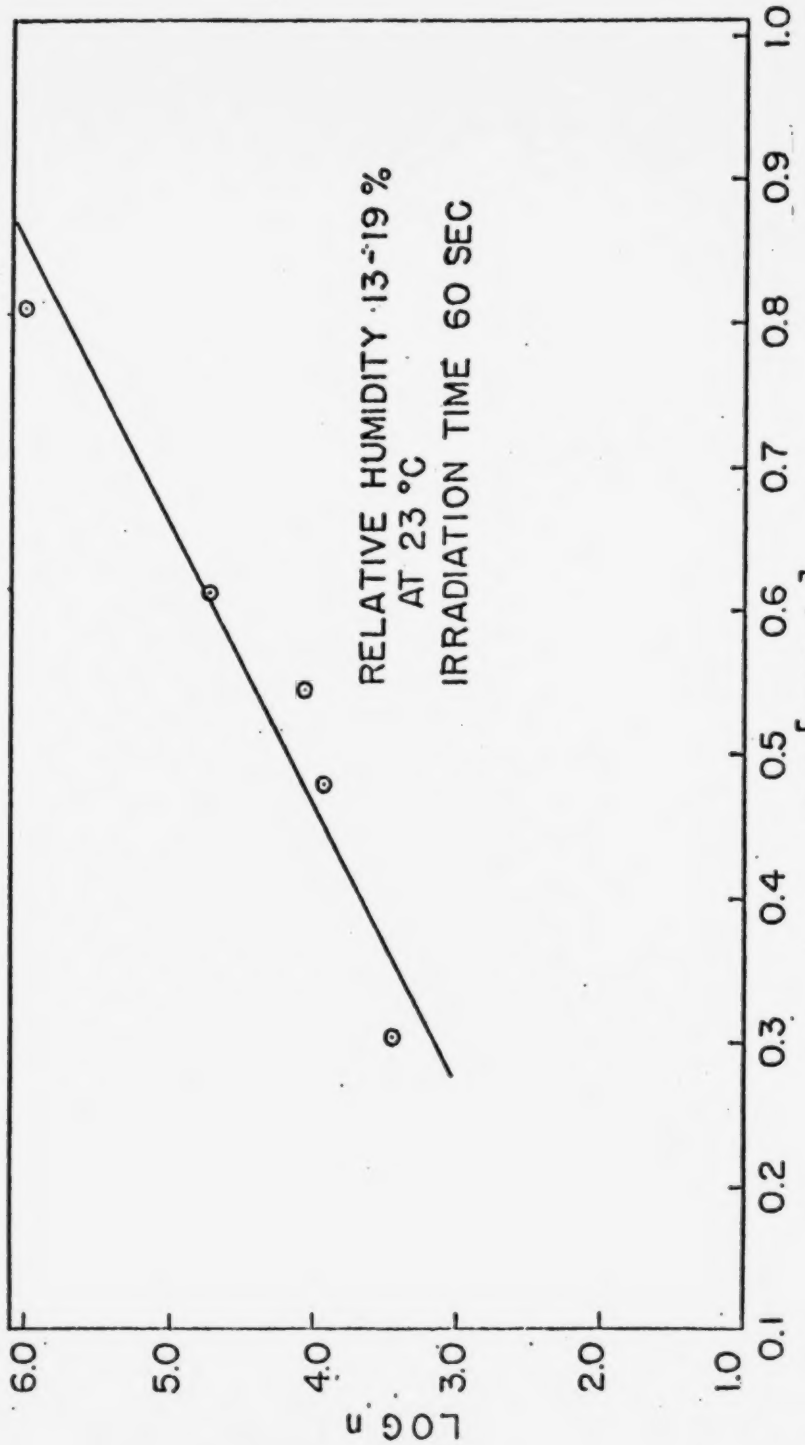

Figure 2. Nuclei Concentration vs Initial Sulfur Dioxide Concentration

Table 1. Nuclei Concentration vs Irradiation Time
(Relative Humidity 13-19%, $(SO_2)_o$ = 0.202 ppm)

Irradiation Time, sec	Nuclei Concentration[a] Average, no./cm^3	Standard Deviation, no./cm^3
30	1,800	1,200
45	3,900	2,800
60	2,600	1,100
90	19,800	12,000
120	33,500	28,600
150	83,900	67,300
180	92,700	81,200
210	140,000	161,000
240	204,000	187,000

a: average of eight separate experiments

Table 2. Nuclei Concentration vs Irradiation Time
(Relative Humidity 41-43%, $(SO_2)_o$ = 0.202 ppm)

Irradiation Time, sec	Nuclei Concentration[a] Average, no./cm^3	Standard Deviation, no./cm^3
30	1,600	350
60	5,000	1,500
120	28,600	7,800
180	97,300	24,300

a: average of eight separate experiments

Table 3. Nuclei Concentration vs Irradiation Time
(Relative Humidity 53-60%, $(SO_2)_o$ = 0.202 ppm)

Irradiation Time, sec	Nuclei Concentration[a] Average, no./cm^3	Standard Deviation, no./cm^3
30	2,600	360
45	7,250	2,758
60	10,800	3,800
90	47,200	19,600
120	84,900	43,100
150	175,000	57,600
180	240,000	34,800

a: average of eight separate experiments

Table 4. Nuclei Concentration vs Irradiation Time
(Relative Humidity 70-77%, $(SO_2)_o$ = 0.202 ppm)

Irradiation Time, sec	Nuclei Concentration[a] Average, no./cm^3	Standard Deviation, no./cm^3
30	6,500	8,200
60	15,400	13,700
120	85,100	44,200
180	235,000	75,300

a: average of eight separate experiments

Table 5. Nuclei Concentration vs Time
(Relative Humidity 49-55%, $(SO_2)_o$ = 0.647 ppm)

Irradiation Time, sec	Coagulation Time Interval, min	Average Nuclei Concentration,[a] no./cm^3	Estimated Nuclei Concentration, no./cm^3
30	8	133,000	
	12	50,000	
	16	25,800	
	20	13,500	10^6
60	8	198,000	
	12	84,700	
	16	50,000	
	20	23,000	10^6
120	12	192,000	
	16	111,000	
	20	70,500	
	24	44,500	10^6
240	12	329,000	
	16	160,000	
	20	91,200	
	24	65,000	3×10^6

a: average of four separate experiments

Table 6. Nuclei Concentration vs Initial Sulfur Dioxide Concentration (Relative Humidity 13-19%, Irradiation Time = 60 sec)

Initial SO_2 Concentration, ppm	Average Nuclei Concentration,[a] no./cm^3
0.202	2,600
0.300	8,200
0.350	14,500
0.410	53,900
0.647	$\sim 10^6$ [b]

a: average of eight separate experiments
b: estimated

Table 7. Nuclei Loss Through Filtration

Filter	Nuclei Concentration[a] Initial, no./cm^3	Effluent, no./cm^3	Percentage Reduction, %
Whatman No. 1	46,000	400	99
	(7,400)[b]	(1,400)	81
Whatman No. 5	34,500	900	97
	(7,400)	(1,500)	79
Whatman No. 40	32,000	300	99
	(7,400)	(1,100)	85
Millipore, type HA (0.45 μ)	34,500	<100	100
	(6,800)	<100	100
Charcoal (13 x 30)	75,000	5,100	93
Molecular Sieve Pellets, type 5A (1/16 inch pellets)	37,000	3,500	95
	(27,500)	(15,800)	43

a: average of five measurements
b: values in parentheses are measurements of room air nuclei concentration

Table 8. Nuclei Loss Through Diffusion Tubes
(Air Flow 3 ℓ/min)

Diffusion Tube	Length, ft	Nuclei Concentration[a] Initial, no./cm^3	Effluent, no./cm^3	Percentage Reduction, %
Tygon, (1/4 in. i.d.)	2	37,000	17,000	54
		(14,400)[b]	(13,200)	18
	4.5	25,500	2,600	90
		(17,000)	(4,700)	72
	6	40,000	3,500	93
		(6,800)	(2,600)	48
	10	34,000	600	98
		(13,200)	(11,000)	17
Rubber, (1/4 in. i.d.)				
Wetted with Alkali	2	25,500	12,200	52
		(17,000)	(14,400)	15
Coated with Alkali	2	34,500	14,400	58
		(8,000)	(6,200)	22

a: average of five measurements
b: values in parentheses are measurements of room air nuclei concentration

SECTION III

A Spark Replica Technique for the Measurement of Sulfuric Acid Nuclei

GENERAL

The association of sulfur dioxide with adverse health effects has been documented by statistical methods of inference[1]. These methods, of course, do not prove the existence of a cause and effect relationship. While considerable attention has been focused on sulfur dioxide as a result of these statistical correlations, very little attention has been given to the measurement of sulfuric acid in the urban atmosphere and its implications to public health. However, the toxicity of sulfuric acid is known to be greater than that of sulfur dioxide and mechanisms of conversion of the dioxide to the acid and methods for the measurement of the acid aerosol are of current interest to individuals engaged in the abatement of air pollution.

Sulfuric acid aerosols may be formed by the photooxidation of sulfur dioxide, and subsequent hydration of the trioxide; the hydration of the trioxide resulting from the combustion of fuel; and the surface catalyzed oxidation of the dioxide. A mass median diameter of $\leq 0.5\mu$ has been reported for the acid aerosol by Waller, et. al.[2,3]. Sulfuric acid aerosol

concentrations of 678 $\mu gm/m^3$ have been observed during periods of atmospheric stagnation[4].

Existing methods for sampling and analysis of sulfuric acid aerosol generally involve collection by filtration, precipitation, or impingement techniques and analysis by titrametric, conductometric, or colorimetric techniques[5-8]. Collection of the acid aerosol on pretreated glass fiber filters and subsequent thermal degradation of the acid to the trioxide and reduction to the dioxide over hot copper enables the use of existing methods of sulfur dioxide measurement for the determination of sulfuric acid in air[9]. The collection of acid aerosol on various types of films and counting the number and size of reaction spots are suitable mainly for the detection and determination of the size distribution of the aerosol[10-12]. Some difficulty in the identification of reaction spots caused by submicron size particles has been reported[13,14].

The spark replica counting technique used for the measurement of nuclear particles [15-17] may be thought to be a variant of the spot reaction method. The adaptation of the spark replica technique to the measurement of sulfuric acid aerosol offers the potential of counting the reaction spots or damage sites of submicron particles without the aid of an electron microscope.

The spark replica method involves exposure of a thin plastic film to a sulfuric acid aerosol and counting the number of defects (holes) in the film. In most applications, the damage sites need to be enlarged by etching the plastic film in a solution of sodium hydroxide for ease of detection. A spark replica counter is used for determining the number of damage sites.

The spark replica counter consists of two charged parallel plates separated by a plastic film. One of these plates is an aluminized mylar sheet. The damage sites on the film function as small capacitors. An impressed electric field of sufficient strength causes the small capacitors to discharge or spark. Each spark may be recorded using a scaler unit similar to those used in connection with a Geiger counter. Each spark causes evaporation of the aluminum film on the mylar adjacent to the damage site. Consequently, each damage site gives rise to only one spark.

The feasibility of adapting the spark replica counting technique for the measurement of sulfuric acid aerosols was explored. A simple spark replica counter was developed and the use of this counter in connection with a sampling system utilizing a polycarbonate plastic film was investigated.

Procedures for the enlargement of damage sites on the plastic film to facilitate counting and different sampling procedures were evaluated. The test sulfuric acid aerosols used for this study were generated by the photooxidation of sulfur dioxide in air. The concentration of the aerosol was measured with a condensation nuclei counter. A relationship between nuclei concentration and spark count was established.

EXPERIMENTAL APPARATUS AND PROCEDURES

Sulfuric acid aerosols were generated by irradiating plastic bags containing a mixture of sulfur dioxide in air, using blacklights with a peak spectral emission at 350 $m\mu$[18]. Gas mixtures of different concentrations of sulfur dioxide were prepared, using the appropriate air flow rates through a mixing chamber containing a sulfur dioxide permeation

tube. The temperature of the mixing chamber was maintained at 23 ^{o}C ± 0.1 ^{o}C.

The concentration of the acid aerosol generated was measured with a Wilson type condensation nuclei meter[19]. The concentration of an aerosol was measured at least three times within a short time period, generally within a three minute period, and the average of the group of measurements was used to represent the concentration of the sample. Each sample removed from the plastic bag does not cause a dilution of the remaining contents. Coagulation and wall losses occur continually, of course.

A spark replica counter consists of the spark chamber, the high voltage power supply, the scaler unit, and the electrical circuit connecting the spark chamber with the scaler. A schematic diagram of the counter is shown in Fig. 1. Picker Compact Scalers (model 60010) were used for the power supply and the scaler unit. One conducting plate of the spark chamber was a sheet of aluminized mylar and the other plate was a flat smooth surface of a block of brass. The dimensions of the brass block were 4" x 1" x 1". As a safety precaution, the brass block was covered with lucite on four of its six faces. A standard post was drilled into one exposed end, and tapped to provide an electrical connection. The remaining exposed surface served as one of the two electrodes of the spark chamber. The counting surface area was approximately 25.8 cm^{2}. The circuit diagram for the counter was established empirically and is shown in Fig. 2. The sizes of the resistors and capacitors were varied until the amplitude of the spark and the time constant of the system was such that each spark was recorded separately by the scaler unit. The amplitude of the output pulse depends on the applied voltage

and was approximately 200 mv at an applied voltage of 550 V. The time constant was about 0.2 μsec. This basic arrangement was patterned after the spark replica counter design used by the Argonne National Laboratory[17].

A plastic film placed between the aluminized mylar and the brass block will act as an insulator. If there are damage sites on the film, each site or hole acts as a small capacitor and will discharge or spark, if a sufficiently high electric field is impressed across the two parallel plate electrodes. An operating voltage in the Geiger plateau region was selected for the counter in order to minimize the dependence of the number of sparks or counts recorded on the operating voltage. As shown in Fig. 3, an applied voltage of 550 volts is suitable.

The suitability of a plastic film for use in conjunction with the spark replica counter for the measurement of sulfuric acid aerosol concentrations depend on the susceptibility of the film to damage by the acid aerosol and on the etching characteristics of the film. Etching the film in a strong solution of sodium hydroxide is necessary to enlarge the damage sites on the film. It is desirable for the thickness of the film to remain uniform and for the film not to buckle after a prolonged etching period. Table I contains a list of several plastic films and a summary of their etching characteristics. Both the 8 and 10μ polycarbonate film (Kimfol) were found to possess good etching characteristics.

Etching the film gives rise to some damage sites on the film. The etching conditions for the polycarbonate film were selected on the basis of convenience and acceptable damage to the film. Fig. 4 shows the spark count or number of damage sites on 8μ thick polycarbonate films, without previous exposure to an acid aerosol, for different etching periods. The

solution of sodium hydroxide used was 6.25 N and the solution was stirred gently at room temperature. Fig. 5 is similar to Fig. 4, but the etching solution was not stirred. After etching, the film was rinsed generously, but gently, in cold water and then rinsed with distilled water. The film was sandwiched between two paper towels and dried in an oven at 100 ^{o}C for 20 to 30 minutes.

Figs. 4 and 5 also show the spark count for polycarbonate films exposed, on a batch basis, to a sulfuric acid aerosol concentration of the order of $10^{6}/cm^{3}$ for 30 minutes. The ratio of spark count for the exposed film to the background count does not increase significantly with an increase in etching time in excess of 12 hours. An etching time of 12 hours was selected to keep the background spark count below 10. The variations in the etching period used were kept within 0.5 hour. The 8μ film was reduced to 6.35μ on the average for this etching period. The decrease of 1.65μ in thickness may be expected to enlarge the damage sites by the same amount, i.e., the dimensional changes are comparable[20].

One side of the polycarbonate film appears duller than the other and this distinction in appearance remained after etching. As a matter of procedure, the dull side of the film was used for exposure to the acid aerosol and was placed facing the brass block of the spark chamber for counting.

Preparation of the film for counting included etching, washing, drying, and subjecting the film to a high electric field (1000 volts per 6.35μ) for a period of 30 minutes. The latter procedure was to develop fully any partially etched holes. The actual counting used an operating voltage of 550 volts. This procedure allowed the counting at 550 volts to be completed in a reasonable length of time.

The method of sampling involved the use of a rectangular diffusion chamber and laminar flow through the chamber. The dimensions of the chamber used were 40.0 cm in length, 5.08 cm in height, and 0.159 cm in width. One wall of the chamber was lined with the polycarbonate film and the aerosol was drawn through the chamber by means of a vacuum pump. Flow rate was measured with a rotameter. Fig. 6 illustrates the sampling system used.

For laminar flow in a rectangular channel, the reduction in concentration of an aerosol is a function of the volumetric flow rate, the diffusion coefficient of the particles, and the dimensions of the channel. In addition to these factors, the number of particles deposited on the channel walls will depend on the sampling period.

A centrally located portion of the exposed film, approximately 25.8 cm^2 (1" x 4"), was used for counting. Each film was counted at least six separate times. Generally, the counts can be replicated within 1%.

Fig. 7 illustrates the number of spark counts obtained for different acid nuclei concentrations, using several sample flow rates. The total sample volume used was kept constant at 1.5 ℓ by varying the sampling period. Coagulation and wall losses were not considered in these measurements since the purposes of these measurements were to determine suitable sampling rates and periods and to assess the approximate spark count to be expected. Coagulation and wall losses were considered in subsequent measurements used to establish the relationship between nuclei concentration and spark count. Fig. 8 shows the spark count for different nuclei concentrations, using several sampling periods and a sampling rate of 150 cm^3/min. A three minute sampling period at 150 cm^3/min was found to be adequate for detecting an acid aerosol concentration of greater than 10^4 per cm^3.

RESULTS AND DISCUSSION

Using the sampling and counting procedures discussed in the previous section, a systematic relationship between sulfuric acid nuclei concentration and spark count was developed. This relationship is illustrated in Figs. 9 and 10. In Fig. 9, each point represents the spark count obtained for a three minute sampling period at a sampling rate of 150 cm^3/min. A semi-logarithmic relation between nuclei concentration and spark count is evident from the information presented in Fig. 9. Four of the points do not follow this relation. If sufficient damage to the polycarbonate film to result in a site giving rise to a spark is caused only by large acid nuclei, then the discrepancies may be attributed to the variation in the fraction of these large acid nuclei in the samples used. However, the reasons for these discrepancies are not entirely clear.

Fig. 10 is a recast of the same information contained in Fig. 9, on an aggregate basis. A cluster of points was represented by the average values of nuclei concentration and spark count for that cluster. Each point was assigned to a particular cluster on the basis of the nuclei concentration associated with the point. In a few cases, the assignment was not defined sharply. The four disparate points were disregarded in developing Fig. 10. The empirical relation illustrated in Fig. 10 is represented by the equation

$$\ln \frac{c}{b} = ms \qquad (1)$$

where

c = sulfuric acid nuclei concentration, nuclei/cm^3,

b = a constant, nuclei/cm^3

m = a constant, per spark, and

s = spark count, sparks.

The values for b and m are 3.4×10^3 nuclei/cm^3 and 0.044 per spark count, respectively. A tabulation of the spark count obtained for each nuclei concentration and the aggregation of these measurements into clusters is given in Table II.

The acid aerosol concentration changes during the sampling period because of coagulation and wall losses. A mean concentration was computed from measurements of nuclei concentration at the beginning and end of each sampling period. Empirically, it was observed that the change in concentration over a short period of time is described by a first order equation with respect to concentration. The concentration corresponding to the middle of the sampling period was defined as the mean concentration.

The reproducibility of the spark count obtained at a nuclei concentration of $10^4/cm^3$ may be estimated from the standard deviation of the nine separate measurements made at this concentration. The standard deviation was found to be 8.6 sparks and is the same magnitude as the background count. Hence, a nuclei concentration of approximately $10^4/cm^3$, corresponding to a spark count of 17 to 25, is the minimum

concentration detectable by the spark replica counter and procedures described here. The sensitivity of the spark replica method for measuring sulfuric acid nuclei was found to be dependent on concentration. For an acid concentration of $10^5/cm^3$, a change in concentration by a factor of two may be differentiated on the basis of the spark counts while for a concentration of $10^4/cm^3$, a change in concentration by a factor of three is necessary.

The number of sparks in relation to the number of acid particles deposited on the film is surprisingly small. As implied by the information presented in Figs. 9 and 10, the ratio is in the order of 10^{-3} One plausible reason for this low ratio is that the formation of a damage site which is sufficiently large, after etching, to cause a spark requires the coincident deposition of two or more acid particles on the same site. It is also possible that only acid particles greater than a certain size are effective in damaging the polycarbonate film. Since the acid particles formed by photooxidation are in the order of 10 $\mathring{A}$[19], it is unlikely that deposition of several particles at the same location on the film occurs frequently enough to account for the ratio of sparks to acid particles.

The development of the spark replica technique for the determination of ambient sulfuric acid concentration requires further information on the specificity of the method and the selection of suitable sampling procedures. Changes in ambient acid aerosol concentration over a sampling period of less than 10 minutes are not significant, although such changes may be large in a laboratory situation. Hence, for atmospheric measurements, the sampling procedures need not be concerned with coagulation. Wall losses in the sampling probe leading to the collector

are easily minimized by the use of relatively large diameter probes and a relatively short length of probe.

The specificity of the spark replica method for the determination of sulfuric acid aerosol concentration depends on the resistance of the polycarbonate film to damage by other acids or substances which may be present in a given sample. The determination of the degree of susceptibility of the film to damage by hydrochloric acid, nitric acid, and various oxidants is pertinent, but was not within the scope of this initial effort.

REFERENCES

1. "Air Quality Criteria for Sulfur Oxides," Natl. Air Poll. Contr. Adm. Publ. No. AP-50, Dept. Hlth. Educ. and Welfare, Washington, D.C., Jan. 1969.

2. Waller, R.E., Brooks, A.G.F., and Cartwright, J., "An Electron Microscope Study of Particles in Town Air," Int. J. Air and Water Poll., 7, 779-786 (1963).

3. Waller, R.E., "Acid Droplets in Town Air," Int. J. Air and Water Poll., 7, 773-778 (1963).

4. Stern, Arthur C., editor, "Air Pollution," Vol. I, 2nd ed., Academic Press, N.Y., 1968.

5. Coste, J.H. and Courtier, G.B., "Sulfuric ACid as a Disperse Phase in Town Air," Trans. Faraday Soc., 32, 1198-1202 (1936).

6. Mader, P.P., Hamming, W.J. and Bellin, A., "Determination of Small Amounts of Sulfuric Acid in the Atmosphere," Anal. Chem., 22, 1181-1183 (1950).

7. Commins, B.T., "Determination of Particulate Acid in Town Air," Analyst, 88, 364-367 (1963).

8. Barton, S.C. and McAdie, H.G., "A Specific Method for the Automatic Determination of Ambient Sulfuric Acid Aerosol," 2nd Int. Clean Air Congress, Int. Union of Air Poll. Prev. Assoc., Washington, D.C., Dec. 6-11, 1970.

9. Scaringelli, F.P., and Rehme, K.A., "Determination of Atmospheric Concentrations of Sulfuric Acid Aerosol by Spectrophotometry, Coulometry, and Flame Photometry," Anal. Chem., 41, 707-713 (1969).

10. Gerhard, E.R. and Johnstone, H.F., "Microdetermination of Sulfuric Acid Aerosol," Anal. Chem., 27, 702-703 (1955).

11. Hayashi, H., Koshi, S., and Sakabe, H., "Determination of Mist Size by Metal Coated Glass Slides," Bull. Natl. Inst. Industr. Hlth, 6, 35 (1961).

12. Horstman, S.W., Jr. and Wagman, J., "Size Analysis of Acid Aerosols by a Metal Film Technique," Am. Industr. Hyg. Asso. J., 28, 523-529 (1967).

13. Lodge, J.P., Ferguson, J., and Havlik, B.R., "Analysis of Micron Sized Particles," Anal. Chem., 32, 1206-1207 (1960).

14. Derre, V. and Pfeifer, H., "Determination of H_2SO_4 Aerosols," Gig. Sanit., 34, 68-69 (1969).

15. Cross, W.G. and Tammasino, L., "Spark Replica Technique for Measuring Neutron Doses with Damage Track Dosimeters," 14th Ann. Hlth. Physics Soc. Meet., Pittsburgh, Penn., June 8-12, 1969.

16. Johnson, D. R., Boyett, R.H., and Becker, K., "Sensitive Automatic Counting of α Particle Tracks and its Applications in Dosimetry," Hlth. Physics, 18, 424-427 (1970).

17. Kastner, J., Private Communication, Argonne National Laboratory, Feb., 1970.

18. Quon, J.E., Siegel, R.P., and Hulburt, H.M., "Particle Formation From Photooxidation of Sulfur Dioxide in Air" 2nd Int. Clean Air Congress, Int. Union of Air Poll. Prev. Assoc., Washington, D.C., Dec. 6-11, 1970.

19. Quon, J.E., "A New Method for the Relative Calibration of a Small Particle Counter," Amer. Industr. Hyg. Assoc. J., 25, 15-24, (1964).

20. Fleischer, R.L. and Price, P.B., "Novel Filter for Biological Materials," Sci., 143, 249-250 (1964).

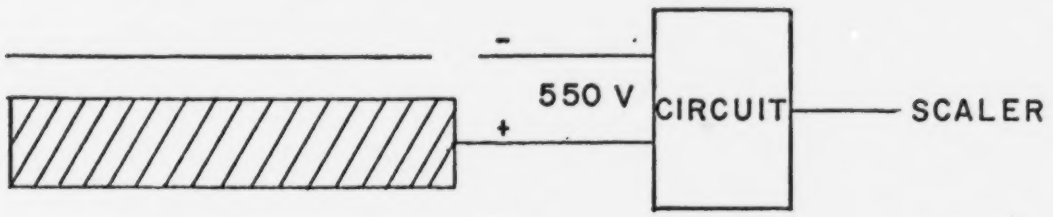

Fig. 1. Schematic Diagram of the Spark Replica Counter.

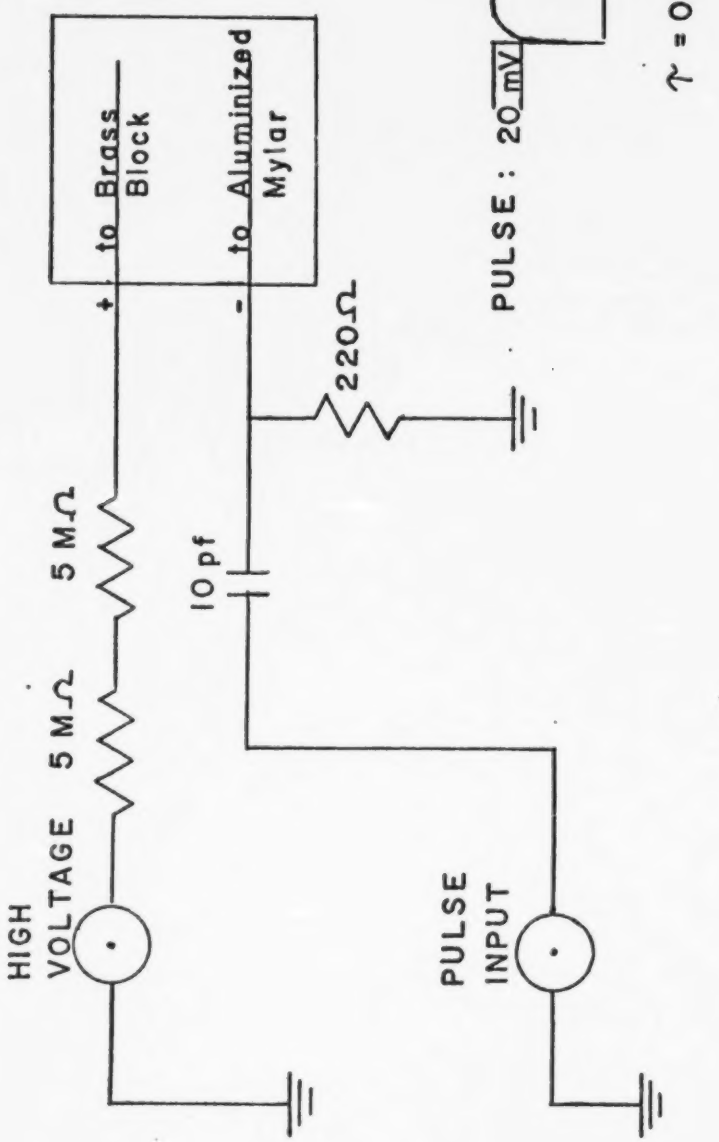

Fig. 2. Electric Circuit Diagram of the Spark Replica Counter.

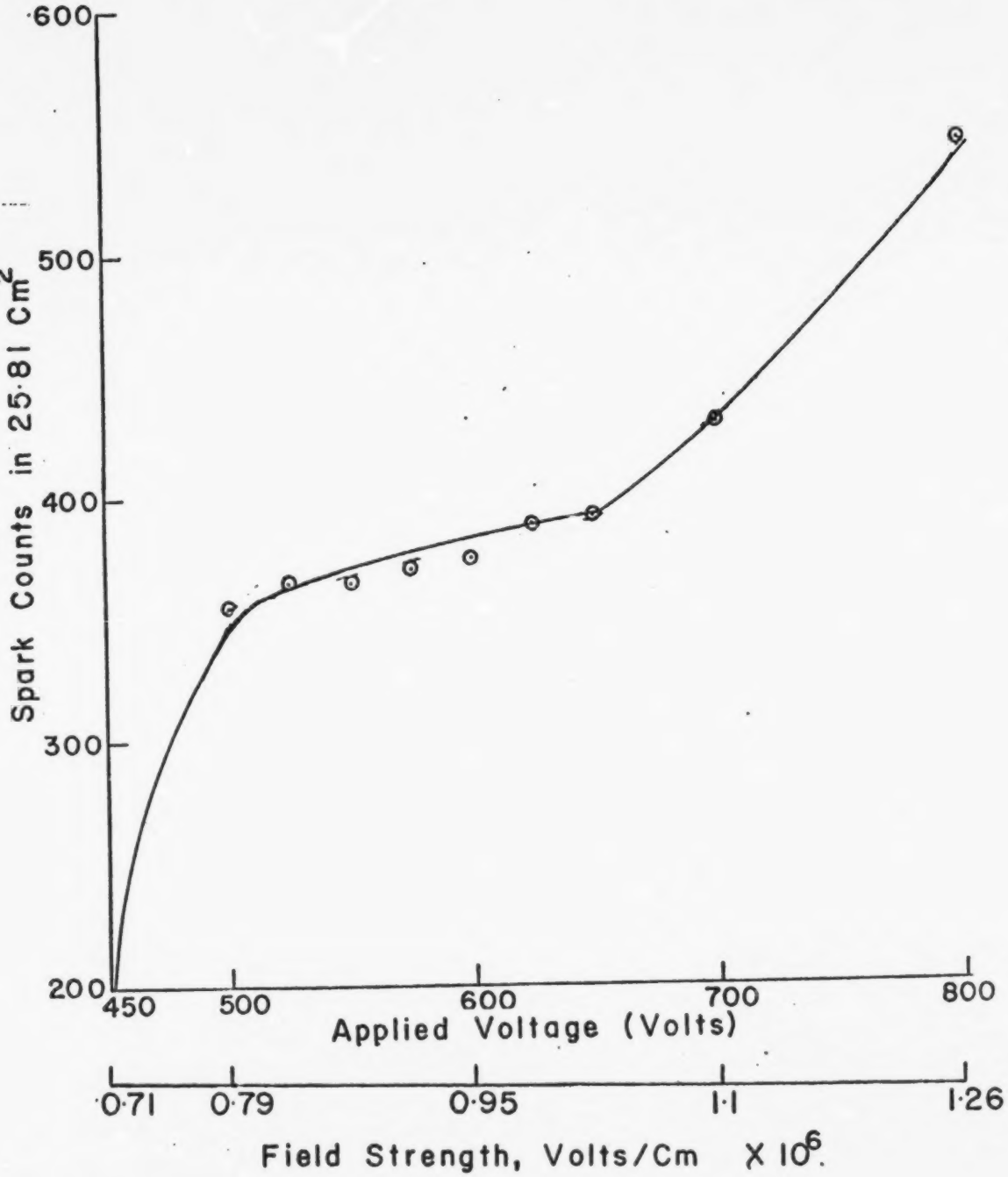

Fig. 3. Spark Count as a Function of the Voltage Gradient.

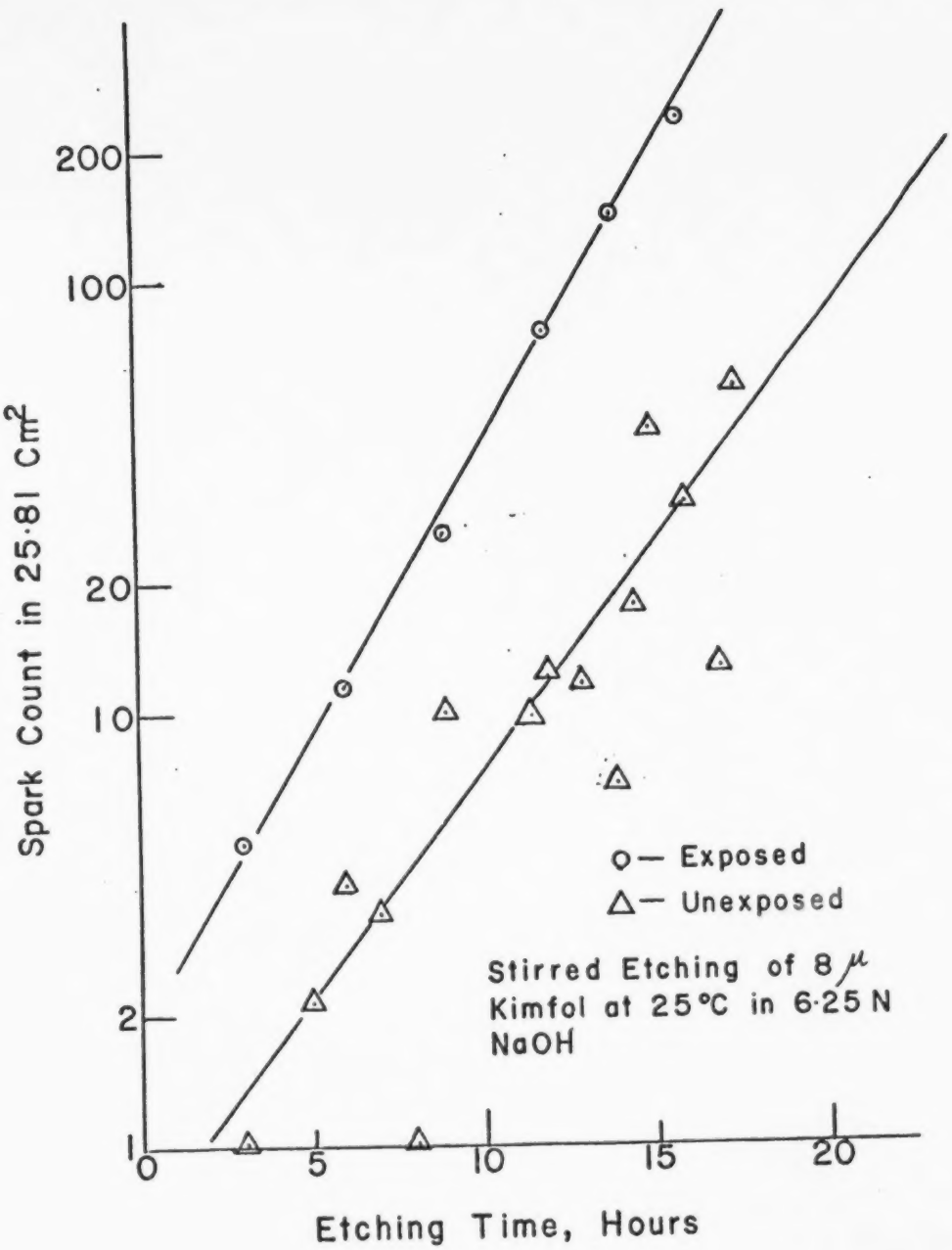

Fig. 4. Spark Count as a Function of Etching Time, With Stirring.

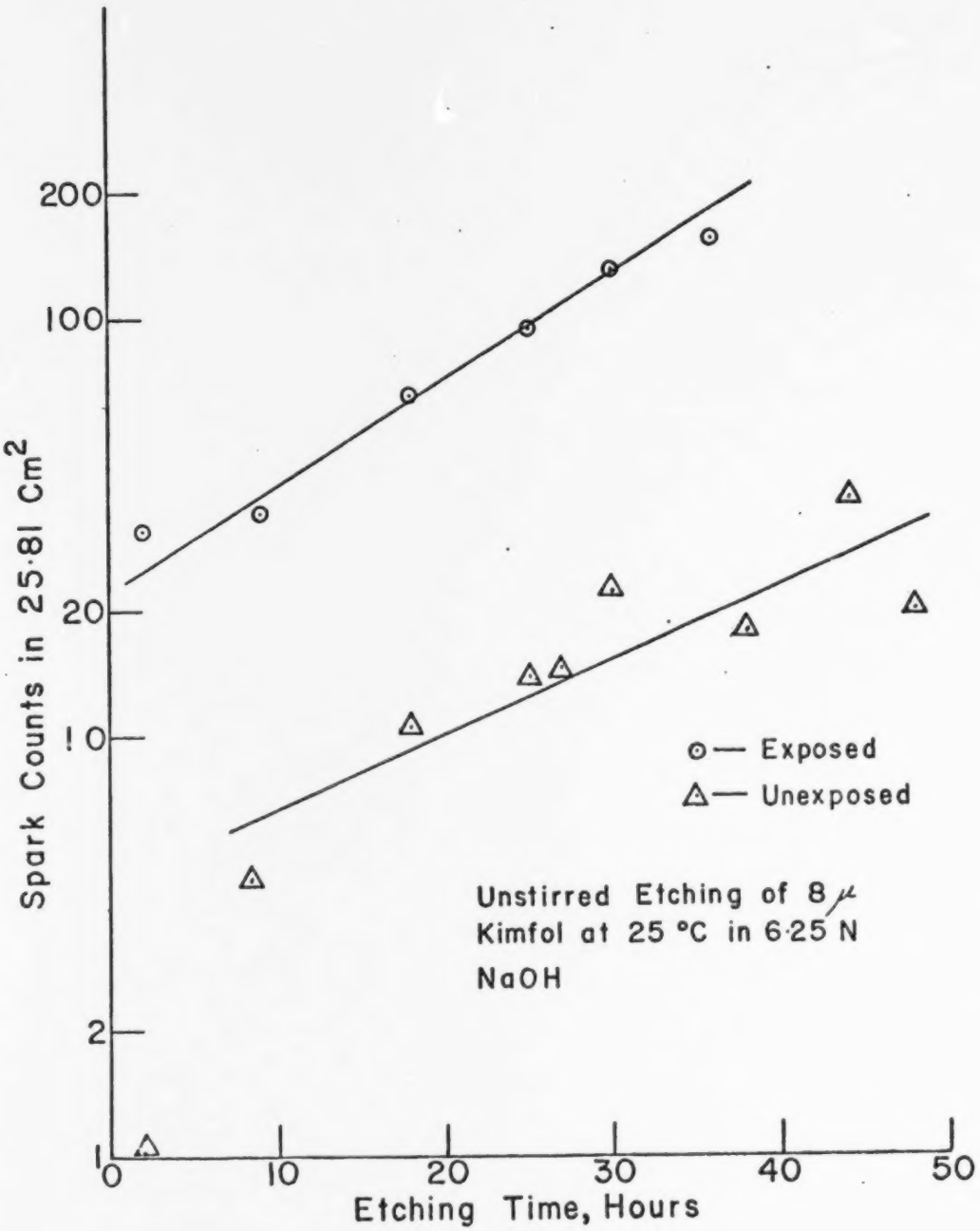

Fig. 5. Spark Count as a Function of Etching Time, Without Stirring.

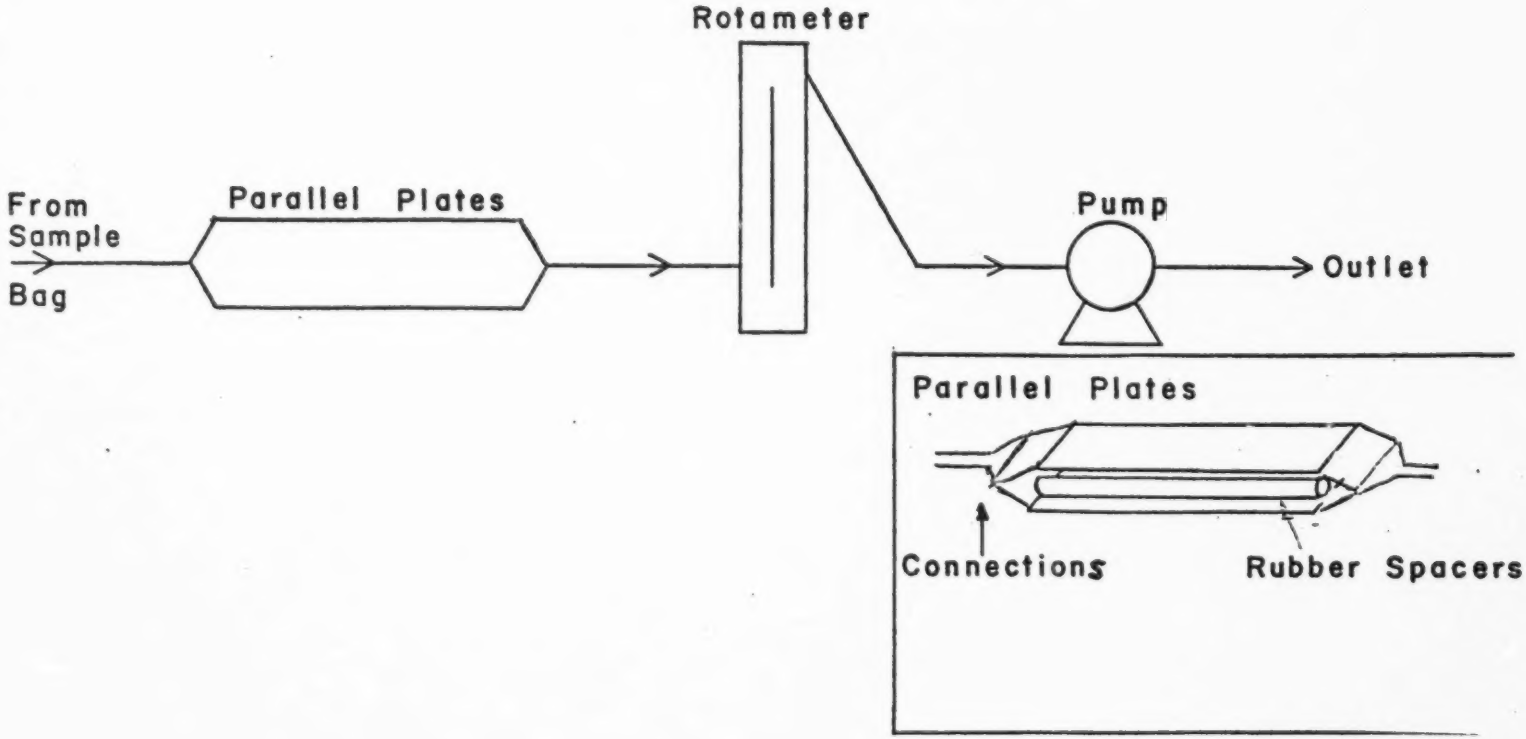

Fig. 6. Schematic Diagram of the Sampling System.

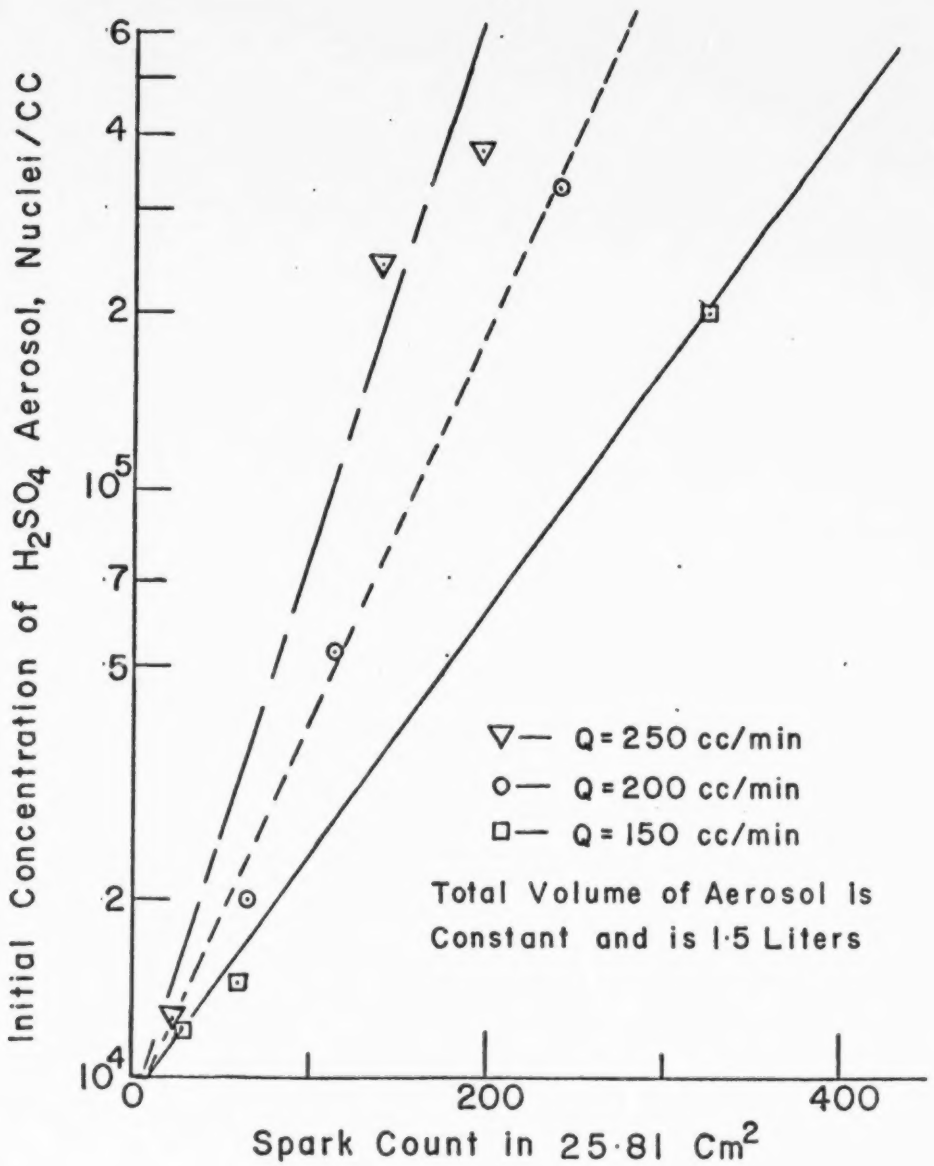

Fig. 7. Effect of Sample Flow Rate on Spark Count.

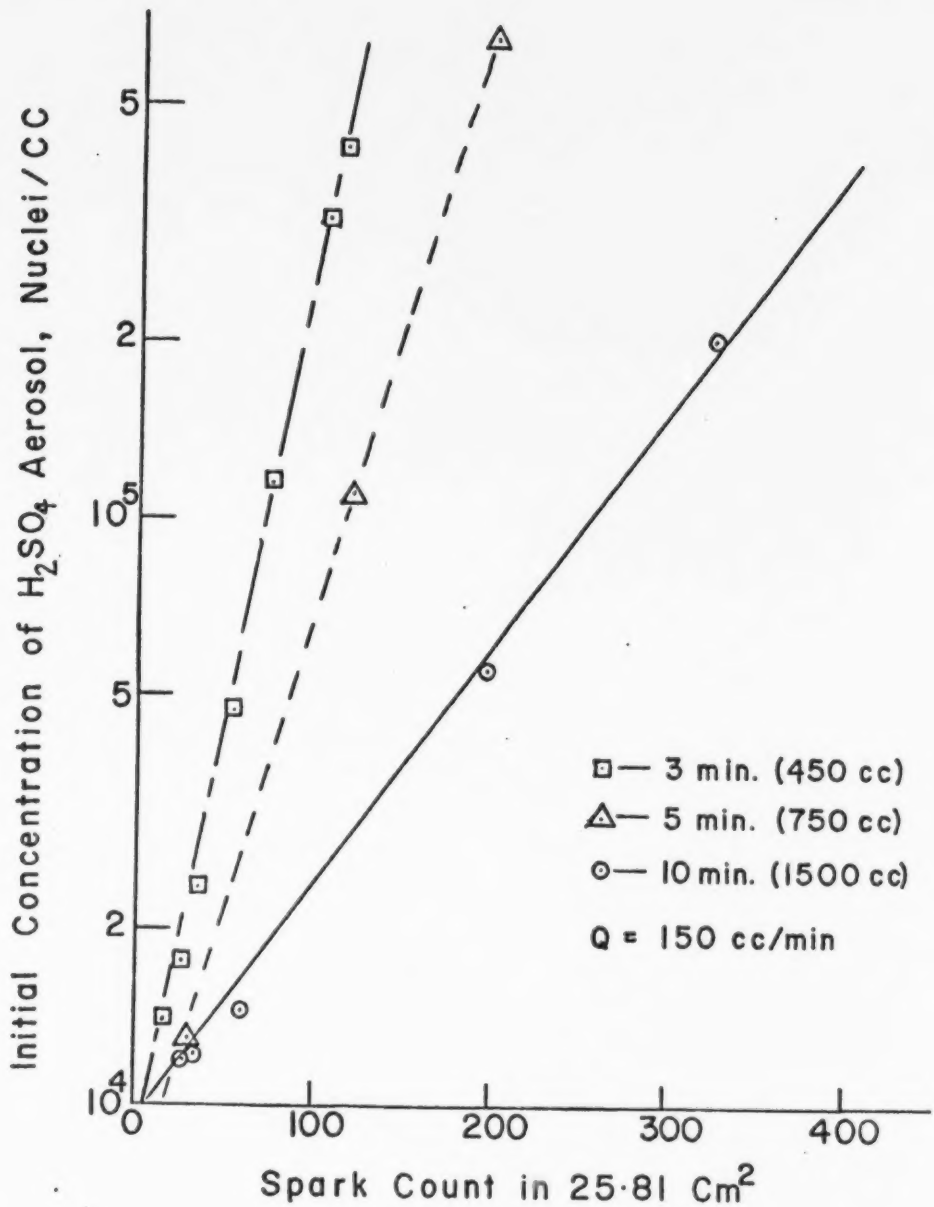

Fig. 8. Effect of Sample Volume on Spark Count.

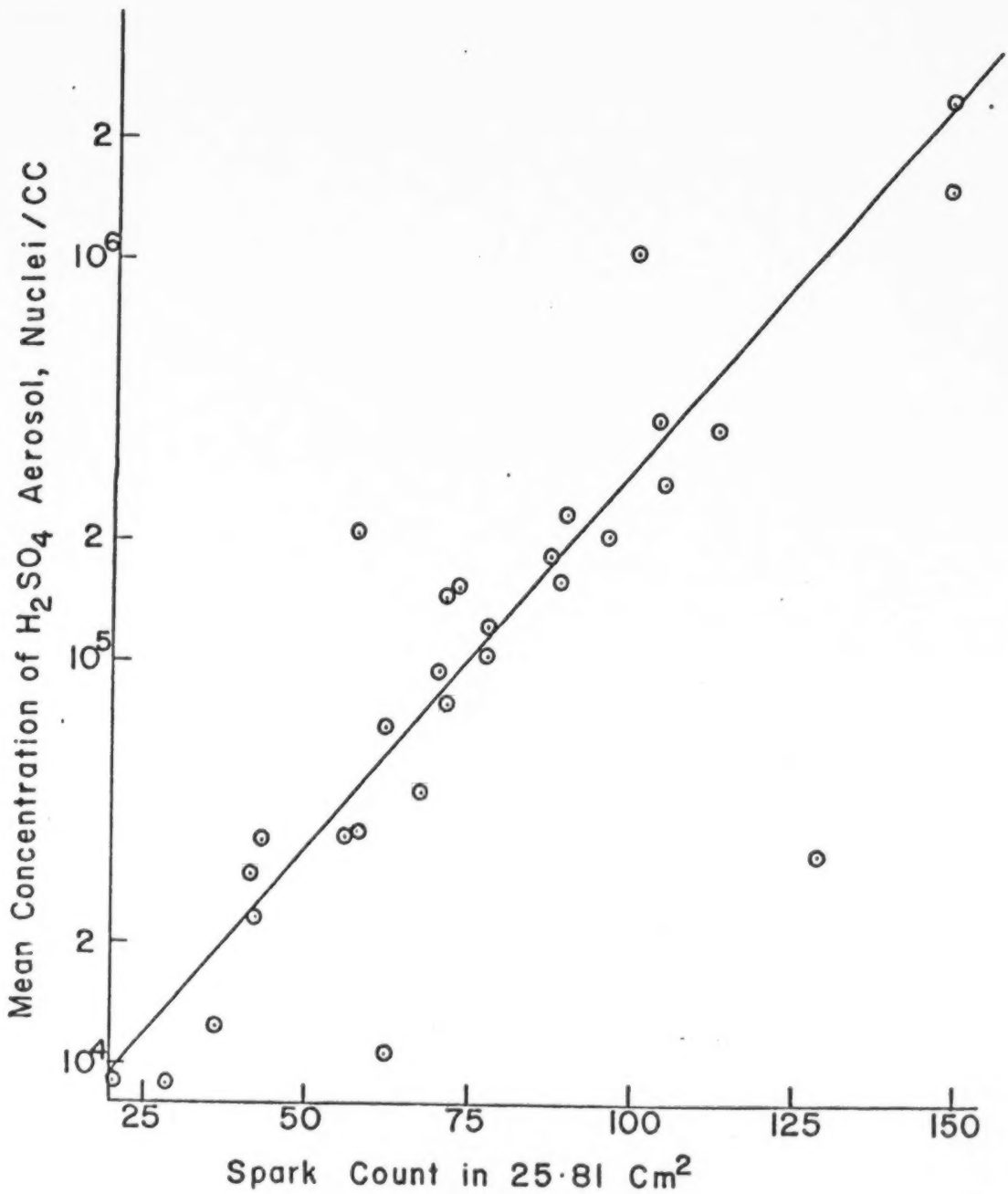

Fig. 9. Nuclei Concentration vs. Spark Count.

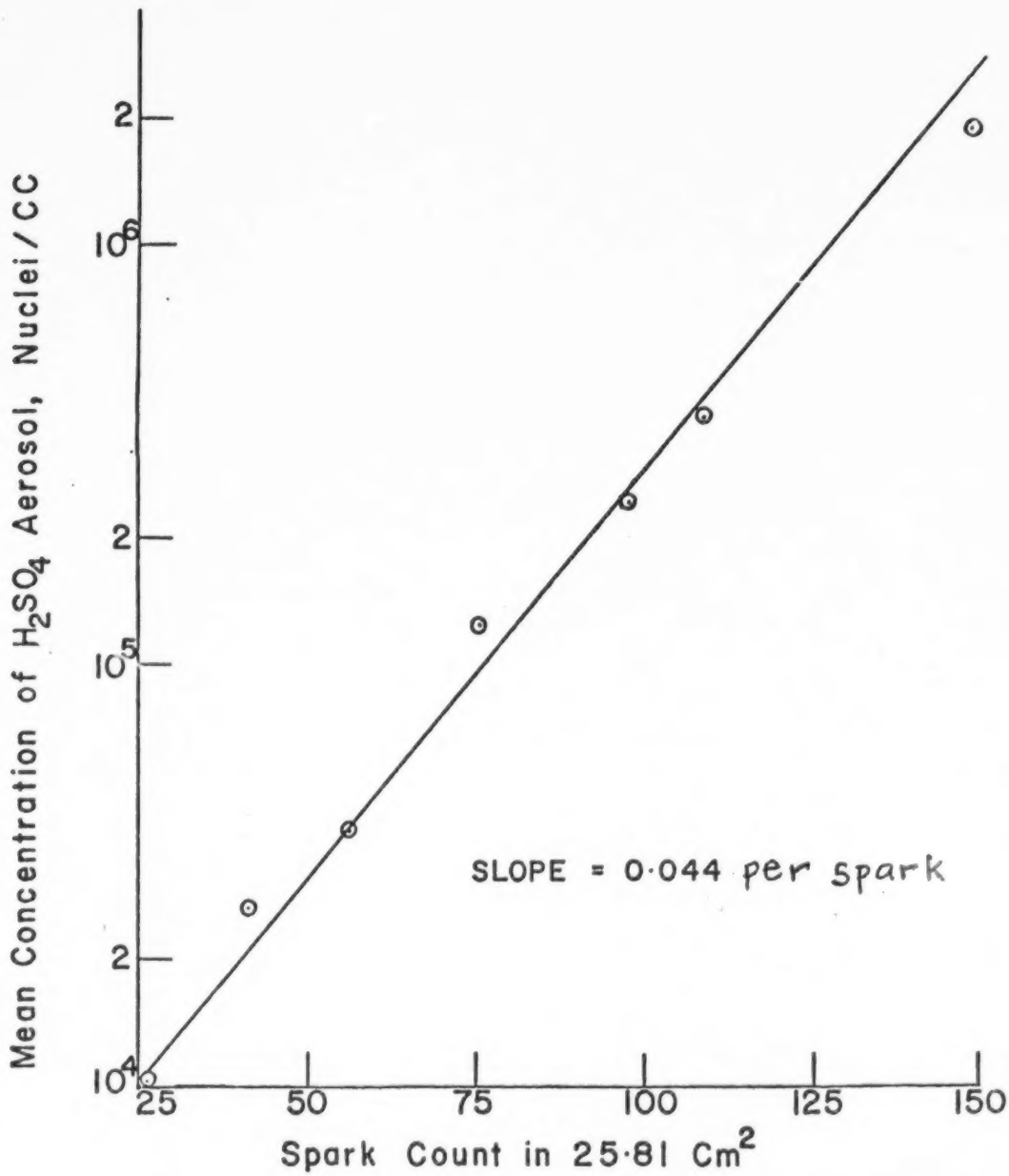

Fig. 10. Nuclei Concentration vs. Spark Count, Aggregated Basis.

Table 1. Etching Characteristics of Plastic Films.

Film	Etching Medium	Etching Period, hrs.	Remarks
Cellophane, coated with cellulose nitrate and various plasticizers	0.5 N NaOH and 1.0 N NaOH	0.5	Sloughing of outer layer; film shrinks and shrivels on drying.
		1.0	Film becomes very brittle.
Cellulose Acetate Butyrate, 0.188"	6.25 N NaOH	12.0	Film curls after etching and is still much too thick to be useful.
Polycarbonate (Kimfol), 8μ and 10μ	6.25 N NaOH	12.0	A flat smooth film results; etching is uniform if film is kept submerged in the etching solution throughout the 12 hours; 8μ film gives much greater spark counts than the 10μ film after exposure to sulfuric acid aerosol.

Table 2. Sulfuric Acid Nuclei Concentration vs. Spark Count.

Run	Spark Count,#	Nuclei Concentration, #/cm³	Cluster Average: Spark Count,#	Cluster Average: Nuclei Concentration, #/cm³
23	28	8.9×10^3	26.2	1.0×10^4
28	18	9.0×10^3		
24	33	1.2×10^4		
30	42	2.3×10^4	41.7	2.6×10^4
38	41	2.9×10^4		
25	43	3.6×10^4	56	4.0×10^4
47	56	3.7×10^4		
48	57	3.8×10^4		
35	68	4.7×10^4		
44	62	6.9×10^4	75.5	1.2×10^5
33	71	7.9×10^4		
26	70	9.5×10^4		
27	78	1.0×10^5	(σ = 8.6)	
31	78	1.2×10^5		
42	71	1.5×10^5		
41	73	1.5×10^5		
43	89	1.6×10^5		
37	87	1.9×10^5		
46	96	2.1×10^5	97	2.4×10^5
36	90	2.4×10^5		
34	105	2.8×10^5		
40	113	3.8×10^5	109	3.9×10^5
29	104	4.0×10^5		
45	148	$\sim 2 \times 10^6$	148	$\sim 2 \times 10^6$
19	148	$\sim 1\text{-}2 \times 10^6$		